การวัดอัตราปริมาณรังสีแกมมาโดยใช้สมาร์ตโฟน

นางสาวสันดี ติด



วิทยานิพนธ์นี้เป็นส่วนหนึ่งของการศึกษาตามหลักสูตรปริญญาวิทยาศาสตรมหาบัณฑิต
สาขาวิชาเทคโนโลยีนิวเคลียร์ ภาควิชาวิศวกรรมนิวเคลียร์
คณะวิศวกรรมศาสตร์ จุฬาลงกรณ์มหาวิทยาลัย
ปีการศึกษา 2558

# MEASUREMENT OF GAMMA-RAY DOSE RATE USING SMARTPHONES

Miss Sandy Tith



A Thesis Submitted in Partial Fulfillment of the Requirements
for the Degree of Master of Science Program in Nuclear Technology
Department of Nuclear Engineering
Faculty of Engineering
Chulalongkorn University
Academic Year 2015

| | |
|---|---|
| Thesis Title | MEASUREMENT OF GAMMA-RAY DOSE RATE USING SMARTPHONES |
| By | Miss Sandy Tith |
| Field of Study | Nuclear Technology |
| Thesis Advisor | Associate Professor Nares Chankow |

---

Accepted by the Faculty of Engineering, Chulalongkorn University in Partial Fulfillment of the Requirements for the Master's Degree

..................................................................Dean of the Faculty of Engineering
(Professor Bundhit Eua-arporn, Ph.D.)

THESIS COMMITTEE

..................................................................Chairman
(Associate Professor Somyot Srisatit)

..................................................................Thesis Advisor
(Associate Professor Nares Chankow)

..................................................................Examiner
(Mr. Decho Thong-aram)

..................................................................External Examiner
(Assistant Professor Attaporn Pattarasumunt)

สันดี ติด : การวัดอัตราปริมาณรังสีแกมมาโดยใช้สมาร์ตโฟน (MEASUREMENT OF GAMMA-RAY DOSE RATE USING SMARTPHONES) อ.ที่ปรึกษาวิทยานิพนธ์หลัก: รศ. นเรศร์ จันทน์ขาว, 84 หน้า.

เป็นที่ทราบกันว่าซีมอสซึ่งตัวรับภาพของกล้องถ่ายภาพในสมาร์ทโฟนมีความไวต่อรังสีแกมมา การวิจัยนี้จึงได้เลือกสมาร์ทโฟน 4 รุ่นมาทดสอบในการวัดรังสีแกมมาจากต้นกำเนิดรังสีอิริเดียม-192 โคบอลต์-60 และซีเซียม-137 ได้แก่ Samsung Galaxy GT-S5570 mini, Samsung Galaxy SII, Samsung Galaxy SIII และ Huawei Ascend P7 ขณะทำการวัดรังสีจะปิดเลนส์กล้องถ่ายภาพด้วยเทปสีดำเพื่อป้องกันแสงแล้วทำการถ่ายภาพในโหมดวิดีโอ อันตรกิริยาของรังสีแกมมากับซีมอสปรากฏเป็นจุดสว่างบนภาพที่มีพื้นหลังมืดจึงเห็นได้ชัดเจน จากนั้นจึงใช้ซอฟต์แวร์ชื่อ ImageJ นับจำนวนจุดสว่างที่เกิดขึ้น ผลการทดสอบขั้นแรกพบว่าจำนวนจุดสว่างที่เกิดขึ้น เพิ่มขึ้นตามอัตราปริมาณรังสีแบบเชิงเส้นสำหรับต้นกำเนิดรังสีทั้งสามชนิด โดยที่ Huawei Ascend P7 มีความไวสูงที่สุดและรองลงมาก็คือ Samsung Galaxy SIII ต่อจากนั้นจึงได้ทำการปรับเทียบสมาร์ทโฟนทั้งสองและทดลองวัดอัตราปริมาณรังสีเทียบกับค่าที่ทราบและค่าที่ได้จากอุปกรณ์วัดอัตราปริมาณรังสี ผลการทดสอบได้ผลเป็นที่น่าพอใจอย่างมาก จากนั้นจึงได้พัฒนาซอฟแวร์ประยุกต์สำหรับสมาร์ทโฟนชนิดแอนดรอยด์ เพื่อให้ทำการนับจุดสว่างที่เกิดขึ้น และแสดงผลเป็นอัตราปริมาณรังสีบนหน้าจอสมาร์ตโฟนได้ทันที



| | | | |
|---|---|---|---|
| ภาควิชา | วิศวกรรมนิวเคลียร์ | ลายมือชื่อนิสิต | ........................................ |
| สาขาวิชา | เทคโนโลยีนิวเคลียร์ | ลายมือชื่อ อ.ที่ปรึกษาหลัก | ........................................ |
| ปีการศึกษา | 2558 | | |

# # 5670577221 : MAJOR NUCLEAR TECHNOLOGY
KEYWORDS: GAMMA-RAY / DOSE RATE / SMARTPHONE / CMOS IMAGE SENSOR / IRIDIUM-192 / CESIUM-137 / COBALT-60

SANDY TITH: MEASUREMENT OF GAMMA-RAY DOSE RATE USING SMARTPHONES. ADVISOR: ASSOC. PROF. NARES CHANKOW, 84 pp.

The CMOS (Complementary Metal Oxide Semiconductor) image sensor of a smartphone has been known for its sensitivity to gamma-rays. In this research, the four models of smartphones (Samsung Galaxy GT-S5570 mini, Samsung Galaxy SII, Samsung Galaxy SIII and Huawei Ascend P7) were selected and tested for measurement of gamma-rays emitted from Iridium-192, Cobalt-60 and Cesium-137 sources. During measurements, the phones were set in video mode while the camera lenses were covered with black adhesive tape to prevent light exposure. Interaction of gamma-rays with the CMOS clearly appeared as flashing bright spots on the dark background image. The bright spots were then counted by the freely available ImageJ software. Preliminary results indicated that the number of bright spots increased linearly with increasing gamma-ray dose rate from these three sources. Among these four models of smartphone, Huawei Ascend P7 gave the highest sensitivity and the second was Samsung Galaxy SIII. Then Huawei Ascend P7 and Samsung Galaxy SIII were calibrated and tested in measurement of gamma-ray dose rate in comparison with the known values and with the dose rate survey meter. The results were very satisfactory. Application software for Android smartphones was finally developed so that the number of bright spots could be simultaneously counted and converted to gamma-ray dose rate to display on the smartphones.

| | | | |
|---|---|---|---|
| Department: | Nuclear Engineering | Student's Signature | ............................ |
| Field of Study: | Nuclear Technology | Advisor's Signature | ............................ |
| Academic Year: | 2015 | | |

## ACKNOWLEDGEMENTS

Firstly, I would like to express my sincere gratitude to my Supervisor Associate Professor Nares Chankow for introducing me to the topic as well as his guidance helped me in all the time of research and writing of this thesis.

Also, I would like to thank the rest of my thesis committee: Associate Professor Somyot Srisatit, Assistant Professor Attaporn Pattarasumunt, and Mr. Decho Thong-aram, for their perceptive comments and encouragement to correct my thesis be completed.

My sincere thanks also goes to the European Commission's CBRN Centers of Excellence for providing me the scholarship of this master program, and thank to Department of Nuclear Engineering, Faculty of Engineering, Chulalongkorn University for giving me the opportunities to study and access my experiment in the laboratory at the department. Also, I thank to the Department of Medical Sciences and the Office of Atoms for Peace for allowing me to access my experiments in their Secondary Standard Dosimetry Laboratories. Without their precious support, I would not complete this research.

I thank my fellow lab mate Miss Nuatawan Thamrongsiripak and Mr. Chalermpong Polee for helping me in experiments and technical discussions, and Miss Tayida Tapjinda for developing the in-house Android application software to test with the real-time counting measurement. Also, I thank my sisters and brothers in the following course of Nuclear Security and Safeguards, and the professors in the Department of Nuclear Engineering for their encouragement.

Last but not the least, I would like to thank my family and friends for their spiritual supporting throughout writing this thesis and my life in general.

**CONTENTS**

Page

Page

# LIST OF TABLES

# LIST OF FIGURES

# Chapter 1

# INTRODUCTION

## 1.1 Background Information

The word “radiation” is known by most people but they do not actually know the meaning. We are always exposed to radiation from the environment mainly from radioactive species present in rocks and soil as well as in the environment and the atmosphere. Gamma-ray is electromagnetic wave like visible light, microwave, radio wave, infrared and ultraviolet. They all travel at the speed of light of 3 x $10^8$ kilometers per second. The major natural sources of radiation are potassium-40 ($^{40}K$), uranium with its daughter radionuclides and thorium with its daughter radionuclides which present in the earth crust. $^{226}Ra$ is a natural radionuclide extracted from uranium ore and was previously used in various applications. However, $^{226}Ra$ has been replaced by man-made radioisotopes such as cobalt-60 ($^{60}Co$), cesium-137 ($^{137}Cs$), iridium-192 ($^{192}Ir$), americium-241 ($^{241}Am$), etc. Working with gamma-ray sources, particularly high activity sources, may give rise to overexposure and cause radiation injury. Radiation dose measurement is of great importance for radiation safety and control. Radiation surveys and continuous record of personal radiation dose are required for all radiation workers.

Nowadays, optical cameras have been replaced by digital cameras which use micro-electronic devices such as CCD’s (charge-coupled devices) and CMOS (Complementary Metal Oxide Semiconductor) as the image sensors. They contain millions of tiny photo sensors. Each of them will create ionized electrons when exposed to light and the current is directly proportional to light intensity. Interaction of the image sensors with radiation can also create ionized electrons. To use digital cameras of smartphones as the radiation detectors is our new challenge especially for measurement of gamma-rays from radiation sources used in industries.

During the past 5 years, CDD has been replaced by CMOS image sensors. Almost all high quality digital cameras are now equipped with CMOS chips. A major advantage that CMOS image sensors more popular is the ability to integrate a number of processing and control functions, which lie beyond the primary task of photon collection, directly onto the sensor integrated circuit. It will be beneficial to radiation workers if their smartphones can be used to measure gamma-rays.

## 1.2 Objective

The main purpose of this study is to use smartphones for measurement of gamma-ray dose rate.

## 1.3 Scopes of Study

1.3.1 Investigation of sensitivity of smartphones to gamma-rays from Cesium-137, Cobalt-60 and Iridium-192.

1.3.2 Calibration of selected smartphones for gamma-rays dose rate measurement.

1.3.3 Measurement of gamma-rays dose rate using the selected smartphones in comparison with those obtained from a calibrated gamma-ray survey meter and the known values.



## 1.4 Benefits

The smartphones can be used to measure gamma-ray dose rate both normal situation such as industrial radiography, and in case of nuclear and radiation accidents such as spillage or dirty bomb explosion, etc.

## 1.5 Research Methodology

1.5.1 The four models of smartphone have been chosen to calibrate with the three gamma-ray sources of $^{192}Ir$ (300-600 keV), $^{192}Cs$ (662 keV), and $^{192}Co$ (1.17MeV and 1.33 MeV)

1.5.2 By using video mode of the back camera of smartphones which lens were covered with the black adhesive tape to prevent exposure to light allowing only gamma-ray to interact with CMOS chip

1.5.3 Each video was converted to pictures by using AOAO video to picture converter software

1.5.4 The number of gamma white spots have been counted by using ImageJ software

1.5.5 The result of gamma-ray dose rate from smartphone was compared with the standard value and dose rate from survey meter.

## 1.6 Literature Reviews

2014 [1], Joshua J., C., D. Kurt W., and W. Jayson were using CMOS sensor in a cellphone for gamma detection and classification. On cellphone processing, the general task of the phone was to filter out various noise sources and determine the approximate doses. By continuously running version of the high delta method, the filter was done. Dose rate was calculated by using a multiplier of the number of pixel that were over a signal threshold value. At the Idaho National Laboratory's (INL) Health Physics Instrument Laboratory (HPIL), the three different model phones were placed in gamma fields produced by $^{60}Co$ and $^{137}Cs$ that the dose rate in the range of 1 mrem/hr to 100000 mrem/hr. the mobile phone model Nexus S was the best for detecting radiation on a per image basis by using CellRad app. Hence this project had concluded that smart phone with a camera could be used as a low sensitivity dose rate survey meter with a known direction, with sufficient data, limited spectrum information.

2014 [2], one research provided by Australian Nuclear Science and Technology Organization (ANSTO), Alison Flynn and her ANSTO colleagues tested the performance of the application software called “Radioactivity Counter” which was designed to measure a person’s exposure to radiation, and now it was available commercially for both Apple and Android devices. So, in this work they used two models of smartphone, the Apple iPhone 4S and the Samsung Galaxy SII. These two smartphones were evaluated using ANSTO’s Instrument Calibration Facility (ICF) which was consisted a range of different dose rates and a movable platform. As a result, both of these smartphones that performed with the Radioactivity Counter software could accurately determine the dose rate which a person is exposed to and it is sensitive enough to detect radiation levels which are significant in a radiological event.

2012 [3], Gumiela, M. and R. Kozik, had written about the applicability of CMOS and CCD sensors for detection, dosimetry and imaging of alpha, beta, gamma, x-ray and proton beam spots. Research result of image sensor response for gamma radiation shown that gamma radiation was investigated for CMOS active pixel sensors from Creative Live! Cam IM pro web camera. With the image mode, it used to detect gamma rays from $^{137}$Cs source that had the radiation activity 2.55 TBq. The main energies of radiation were 660keV and 30 keV. The image sensors were more sensitive to lower energy of radiation. Gamma photons of 30 keV were mainly detected. The number of traces were counted by using dedicated software. Also, by using LG KU250 mobile phone to capture the image of $^{137}$Cs was done. The phone with special software could detect dose rate from 3 mGy/hr until the lower detectable dose rate 232 μGy/hr. it was shown that a mobile phone with a special software could be used as an alarm against the risk of gamma radiation.

2012 [4], a thesis research about Development of an Iridium-192 Gamma Radiography System Using PI-200 Fluorescent Screen Coupled with Digital Camera was done by Mr. Kittiwin Iemsumang. By using gamma-ray sources of Selenium-75 ($^{75}$Se) and $^{192}$Ir to investigate the gamma radiography system. In the experiment, the author developed an image viewing system by using Kyokko PI-200 Fluorescent screen to transform transmitted gamma-ray intensity to light and the digital camera with CMOS chip that connected to a microcomputer via USB port. The result was shown that the CMOS chip inside the digital camera interacted with gamma radiation by having the bright spots on image. However, in this thesis work, the author worked on development of radiography, so he used ImageJ software to count the bright spots (noise) and used many techniques to remove those noises.

2011 [5], IEEE International conference reprinted with permisssion from Low Cost, Pervasive Detection of Radiation Threats, in Technology for Homeland Security (HST) decribed the use of technology in calibration and testing scenarios using installed video cameras and smartphone cameras. With the GammaPix technology, developed at Advanecd Fuel Research, Inc. (AFR) was operated on the digital images produced by a surveillance or smartphone camera to measure the local gamma ray radiation exposure at the device. This technology had been tested with many different cameras include surveillance camera, smarphones, and webcam, and the sensivity of its system depends on the physical size of the CCD or CMOS chip present in the camera. For smarphone, the initial version was developed for Android platform, and many models of smartphone had been carried out calibration experiments by National Institute of Standards and Technology (NIST) on nuclear accident at the Fukushima Daichi nuclear plant. The result was shown that the GammaPix system has been successfully tested at NIST by showing the response curve was linear over a wide range of radiation dose rates.

2001 [6], Munir A. Abdalla did a thesis in Sweden about pixel detectors and electronics for high energy radiation imaging. They had designed several CMOS read-out electronic chips for dental x-rays imaging such as CMOS APS for bump-bounding to a semiconductor pixel detector, CMOS APS coated with a scintillation layer and integrating CMOS APS for x-ray imaging with an in-pixel preamplifier. The main accent was on the direct x-rays absorption and sensitivity of these devices. So, these methods could prove the CMOS technology to replace the CCDs perfectly.

# Chapter 2

# PRINCIPLES AND THEORIES

## 2.1 Gamma Rays

### 2.1.1 Definitions and Properties of Gamma Rays

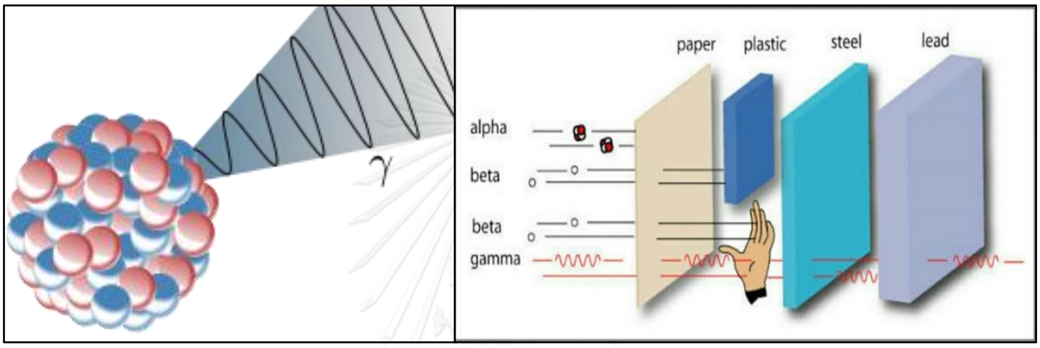


*Figure 1. Gamma ray (source: www.en.wikipedia.org) and its interaction with materials (source: www.frankswebspace.org.uk)*

Gamma rays are high-energies of electromagnetic radiations (they have both electric and magnetic properties) that are emitted from the nuclei of excited atoms, weightless packets energy, and they are pure energy. The gamma rays wavelengths are shorter than 0.10 Å, but the frequency of gamma rays lies about 10 EHz. These radiations travel through the vacuum with the speed of light and formed as a continuous spectrum, which have widely different energies in the range of 0.010 MeV to 17.6 MeV. The radiations are originated from the natural decay reactions of radioactive nuclides and they are also the productions of manmade reactions.

$$I = I_0 e^{-\mu t}$$

Which, $I$ is the intensity of transmitted gamma rays

$I_0$ is the intensity of incident gamma rays

$\mu$ is linear attenuation coefficient ($cm^{-1}$)

$t$ is the thickness of the material

Furthermore, gamma photons produce ionization indirectly and their interaction processes are described by the three major effects as Photoelectric Effect (photoelectric emission or Photoemission) which is an interaction can happen when a gamma photon can eject an orbital electron from an atom, and the electron will take up all the energy of the photon then the photon disappears completely. It exists archly with gamma photons of energy less than 0.511 MeV. The probability of photoelectric effect depends on the electron binding energy, the atomic number of atom, and the energy of gamma-ray. The importance of photoelectric absorption is for gamma-ray detection because all the energy of gamma-ray will transfer to the freed electron and the result is shown in full energy peak. The second interaction is Compton scattering which is the scattering interaction is occurred when the photon energy is large enough, and gives up part of its energy to an electron. The same as photoelectric effect, the freed electron is ejected and cause ionization. Furthermore, another gamma photon of lower energy will take away the remaining energy and travel in a new direction. Later this scattered photon can be absorbed by the photoemission with another atom. The probability of Compton scattering depends on the electron density, the atomic number of atom, occurs in all materials, and exist with gamma photons of energy from about 0.511 MeV to about 3.00 MeV. And the third one is Pair Production which is an interaction that a high energy gamma photon of at least 1.02 MeV can produce an electron-positron pair and it cannot happen with the energy less than this 1.02 MeV. However, pair production can occur only near the nucleus of an atom. This interaction is described in the process of the conversion of energy to mass, which the photon energy is share equally by the positron and the electron. And the way to cause the ionization is the same as the electron do in the photoelectric emission and Compton scattering. On the other hand, both electron and positron from the pair production are quickly slowed down and the positron is ended up by being captured by an electron. Then the pair convert to two new photons which have an energy of 0.511 MeV each, this process called annihilation. So, both energies will be absorbed by the photoelectric effect or scattered by Compton Effect.

All in all, whether gamma rays interact with matter in terms of pair production, Compton scattering or photoelectric effect, the final result must be the product of electrons and positive ions. And in case of the matter is the human body, they can cause ionizations and all tissues will be exposed to injury.

Also, shielding from gamma rays is necessary to use the materials with high atomic number and high density. The higher the energy of gamma rays, the thicker the shielding made from the same shielding material is required. The effectiveness of material for shielding gamma rays is measured by the Half-Value Layer (HVL), which is the thickness of absorber required to reduce the gamma ray to half its former intensity. [7], [8], [9], [10]

HVL = $\frac{ln2}{\mu}$ and

nHVL= $(\frac{1}{2})^n$ of the original

Note: 7 HVLs reduce the radiation field less than $\frac{1}{100}$ or 1%

10 HVLs reduce the radiation field less than $\frac{1}{1000}$ or 0.1%

### 2.1.2 Applications of Gamma Rays

In radiation technology, gamma radiation is one of the most important radiation that is used in many radiation processing applications such as:

Medical Treatment Applications: gamma rays are used to kill or control the certain types of malignant tumors and cancers in the body. The rays are employed as a gamma knife to damage the cancerous cell’s DNA, causing them to die or slow down their reproduction. Gamma rays are also used to detect brain and cardiovascular abnormalities, and sterilize equipment as an alternative to chemical treatments.

Medical Diagnostic Applications: Although gamma rays can be emitted in different ranges of energy, as a diagnostic tool gamma rays might be emitted on the same energy range as x-rays. The patient is injected the gamma radioactive tracer and a gamma camera is then used to form an image of the tracer’s distribution in the body by mapping the gamma rays. The image from the camera can be used to diagnose a number of conditions from the distribution of the patient’s symptoms.

Radiation Imaging: Although x-rays have been used in imaging test, specialized gamma ray scanning equipment is used to get a high-quality diagnostic image. The patients ingest liquids containing gamma-rays emitting substances then the scanner detect the gamma radiation in the body and create three dimensional diagnostic images of functional processes in the body. This procedure is known as Positron Emission Tomography (PET scan).

Industrial Applications: Gamma radiations are used in many industrial applications. Industrial radiography is one of the longest established industrial applications of radiation for the non-destructive testing of items of equipment. This application process supply a method of proving the physical integrity of equipment and structures such as examine metallic castings or welds in oil pipe lines for weak points. Furthermore, gamma rays also are important for food industry in the ways of sterilization and irradiation.

Science and Researching Application: gamma radioisotopes are used as tracers in many research areas on most physical, chemical and biological systems treat radioactive and non-radioactive forms of an element in exactly the same way. [11], [12]

### 2.1.3 Commonly Used Gamma Emitting Isotopes

Radionuclides which emit gamma radiations are valuable in a range of different industrial, scientific, and medical technologies. There are many commonly used gamma radioisotopes such as:

Cobalt-60 [13], [14]: it is one of the major radioactive cobalt isotopes that is produced commercially through linear acceleration for use in medicine and industry. It is also byproduct of nuclear reactor operations. $^{60}$Co is a hard, gray-blue metal which forms as solid material and might appear as small metal disks. It is also can form as a powder if the solid sources have been grounded or damaged. The half-life of $^{60}$Co is about 5.3 years by emitting a beta particle with two energetic gamma rays (the total energy of gamma rays is about 2.50 MeV which one has an energy of 1.17 MeV and the other has an energy of 1.33 MeV). $^{60}$Co makes an important usages to the health and well-being of people, as well as providing significant benefits to many industries around the world. It is used medically for radiation therapy as implants and as an external source of radiation exposure. In addition to these important health care applications, $^{60}$Co is also used for material modification processes such as the cross-linking of polymer chains, creating longer molecular bonds or chain-scission for shorter polymer chains. Furthermore, in industries it is used in leveling gauges and to x-rays welding seams and other structural elements to detect flows. $^{60}$Co plays an important role in the scientific community as well, from promising new stem cell research to the design and testing of components for the aerospace and nuclear energy industries. And other beneficial uses include food preservation, decontamination of packaging materials, sanitization of cosmetics, microbial reduction in pharmaceuticals and quarantine application of consumer products.

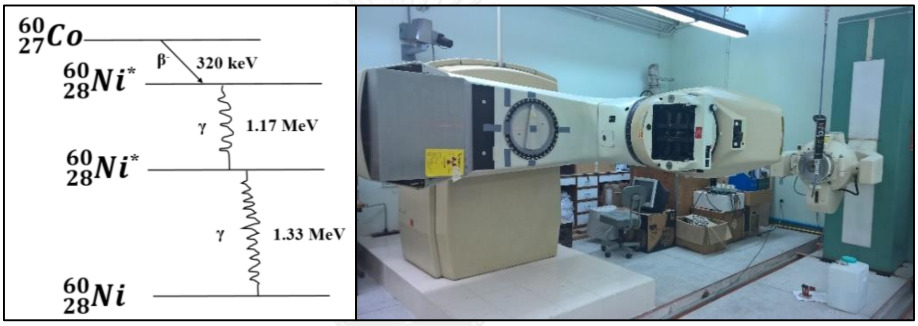


*Figure 2. Decay scheme of $^{60}$Co and $^{60}$Co source in teletherapy machine*

Cesium-137 [14]: It is one of the byproducts of nuclear fission processes in nuclear reactors and nuclear weapons testing. It is also found in spent nuclear fuel, high level radioactive wastes resulting from the processing of the spent nuclear fuel and radioactive wastes associated with the operation of nuclear reactors and fuel reprocessing plants. $^{137}$Cs usually form as a crystalline powder, rather than in its pure liquid form. The half-life of $^{137}$Cs is about 30 years. Its decay product, $^{137m}$Ba stabilizes itself by emitting an energetic gamma ray of 662 keV. The small amount of $^{137}$Cs is used for calibration of radiation detection equipment in calibration facilities. In larger amounts, this gamma source can be used in medical radiotherapy devices for the treatment of cancer. It is also used in industrial gauges that detect the flow of liquid through pipes, in food irradiation, and other industrial devices to measure the thickness of materials such as paper, photographic film or sheets of metal. However, $^{137}$Cs is not widely used for industrial radiography because it is quite chemically reactive, and it is also difficult to handle.

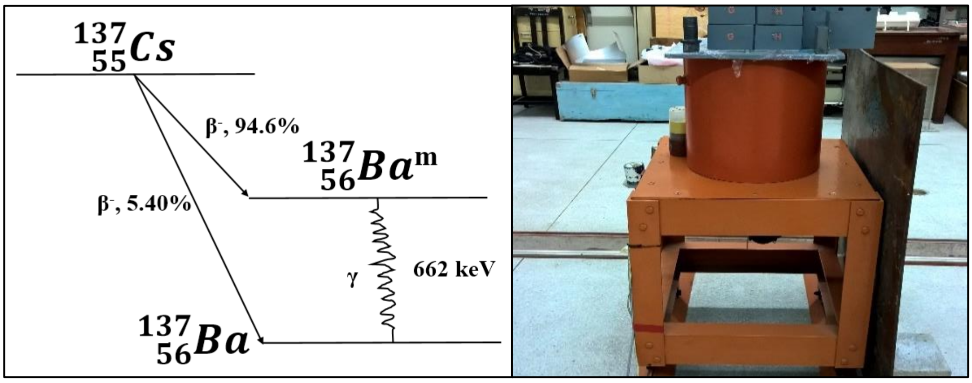


*Figure 3. Decay scheme of $^{137}Cs$ and $^{137}Cs$ source in shielded container in laboratory*

Iridium-192 [15], [16]: is normally produced by neutron activation of natural-abundance iridium metal, usually in nuclear reactors. The specific activity of a resulting $^{192}$Ir is related to the amount of neutron irradiation and length of time to which the natural-abundance iridium metal is exposed. During irradiation, only the stable isotope $^{191}$Ir is activated to produce $^{192}$Ir by absorbing a neutron. The half-life of radioactive $^{192}$Ir is about 73.8 days. This radioactive is used principally for non-destructive testing (NDT) and to a lesser extent, as a radio-tracer in the oil industry. Furthermore, $^{192}$Ir is basically used for industrial gamma radiography involves the testing and grading of welds on pressurized piping, pressure vessels, high-capacity storage containers, pipelines, and certain structure welds, other tested materials include concrete, machined parts, plat metal, and pipe wall. This gamma radiography is also used to identify flows in metal castings and welded joints, as well as to indicate structural anomalies due to corrosion or mechanical damage. Moreover, $^{192}$Ir is used in the production of radioactive "sealed sources" that emit a focused beam of $^{192}$Ir gamma radiation on a target testing materials. For medical application, $^{192}$Ir is also used medically in brachytherapy (brachytherapy is a method of radiation treatment in which sealed sources are used to deliver a radiation at a distance of up to a few centimeters by surface, intracavitary or interstitial application) to treat various types of cancer. This gamma source implants are also used, especially in the head and breast. They are produced in wire form and introduced through a catheter to target area. After being left in place for the time required to deliver the desired dose, the implant wire is removed. This procedure is very effective at providing localized radiation to the tumor site while minimizing the patient's whole body dose absorption.


*Figure 4. $^{192}$Ir source in shielded container*

Selenium-75 [15] [17]: the elemental selenium is highly toxic, volatile, reactive and corrosive. Early source designs containing elemental $^{75}$Se had to contain some void space inside the capsule to allow for this expansion during reactor irradiation when the selenium melted. Its half-life is about 120 days. The source design is referred to as the $^{75}$Se$^{ntinel}$ source and has been designed by Sentinel$^{TM}$ to meet the needs for the more double, thermally stable, high performance product, in response to market needs. A thermally stable compound of a non-activating metal combined with selenium is used in the capsule. The engineered cavity in the capsule determines the shape of the focal geometry. The capsule can be made available in either titanium or vanadium. In application, gamma radiography using $^{75}$Se is now generally acknowledged throughout the world to provide performance benefits relative to $^{192}$Ir in the working range of 5.00-30.0 mm steel. $^{75}$Se has a softer gamma ray spectrum than $^{192}$Ir and it has a significantly longer half-life. For gamma radiography, it is required the use of compact, robust, high activity sources with small focal dimensions. It has been particularly successful in replacing x-ray devices in some pipeline crawler applications. And the advantages of longer half-life, improved operator safety, smaller exclusion zone and high image quality can be used more in remote geographical regions and most particularly in offshore applications if compare with $^{192}$Ir and $^{169}$Yb.


*Figure 5. $^{75}$Se source in shielded container and the structure of capsule of $^{75}$Se. Source: www.ndt.net*

Ytterbium-169 [18]: it is one of the most stable radioisotope of ytterbium with a half-life of 32.0 days. $^{169}$Yb is created along with the short-lived $^{175}$Yb isotope by neutron activation during the irradiation of ytterbium in nuclear reactors. This radioactive source has been used in portable x-ray machines, and its gamma rays are emitted by the source pass through soft tissues of the body, but are blocked by bones and other dense materials. Moreover, the small amount of $^{169}$Yb which emit gamma rays act like tiny x-ray machines are useful for radiography applications. In medical application, $^{169}$Yb is used for intravascular brachytherapy (IVBT) in terms of dose distribution, penetration power, and radiation safety features as compare with $^{125}$I and $^{192}$Ir.

Iodine-131 [19]: is an important radioisotope of iodine which is produced from nuclear reactor neutron-irradiation of natural tellurium target. Its half-life is about 8.00 days. $^{131}$I is also one of the most commonly used gamma-emitting tracer isotopes are injected with hydraulic fracturing fluid to determine the injection profile and location of fractures created by hydraulic fracturing. And this radioactive tracer is a great importance in nuclear medicine, and in medical and biological research. This isotope is not of practical use in radioactive sources in industrial radiography or sensing because about 90% of radiation is beta radiation causes tissue damage without contributing to any ability to see in image.

2.1.4 The Danger of Gamma Radiation

Although gamma radiation have many significances in application, it always harm people in dangers. Gamma rays are forms of ionizing radiation; these rays and particles can cause chemical and physical damage when they deposit energy in human tissues. We can be exposed to gamma rays from three main sources: natural background radiation (it comes from cosmic rays and radioactive elements), medical radiation (by using imaging tests and radiation therapy) and non-medical or man-made radiation (is found in food irradiation, airport security scanners and in some materials. It can be happened in both controlled and uncontrolled area as a result of nuclear accident or nuclear weapon testing). The health effects resulting from exposure to radiation can cause to death and disorders. Gamma radiation can cause as external, internal and skin contamination exposure.

For external exposure, it occurs from sources outside the body such as in medical testing equipment and from the dust or rocks.

Also internal exposure, it is occurred when radioactive material get inside the body through inhalation, absorption or ingestion. Gamma rays can pass completely through the body and the fraction will always absorbed by tissue.

And skin contamination, is refer to something that occur by radioactive materials are accidentally spilled on the skin. For gamma emitters can also deliver a skin radiation dose; in addition, they maybe a hazard to other body tissue.

We divide radiation exposure into two terms: short-term (acute) and long-lasting (chronic). Acute whole body radiation overexposure affects all the organs and systems of the body. Hence it can be caused as radiation sickness (acute radiation syndrome) and even death. The three classes of acute radiation syndrome are: the hemopoietic syndrome, the gastrointestinal syndrome and the central nervous system syndrome. The certain effects are common to all categories; these include fainting, confusion, nausea and vomiting, diarrhea, hair loss, skin and mouth sores, bleeding and even the children of pregnant women who were exposed to high doses of radiation have shown an increased risk of birth defects. On the other hand, gamma rays are also known as human carcinogens. People who expose to high doses of radiation from atomic bomb testing, nuclear accident, people treated with high doses of radiation for cancer and other conditions or some people expose to high levels of radiation at workplace, all of these can cause to cancer and genetic mutations. [10], [20], [21], [22]

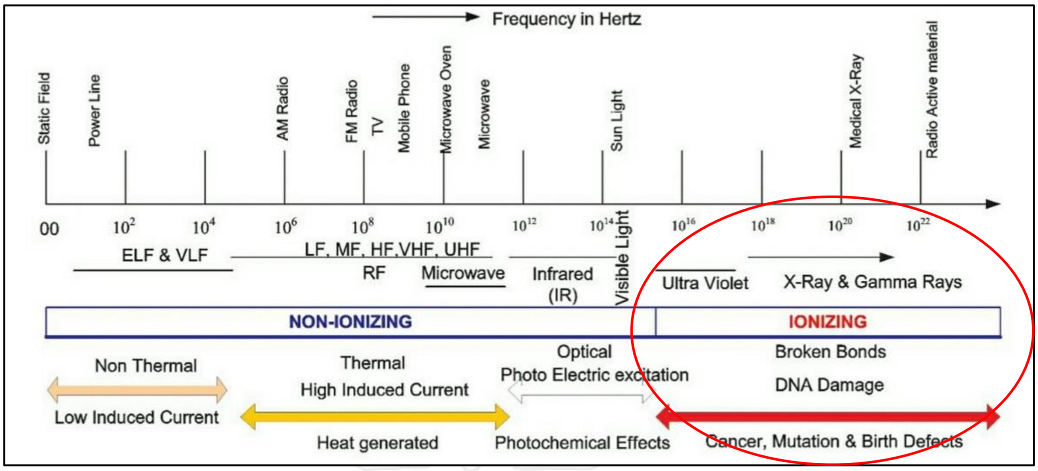


*Figure 6. The diagram of gamma ray spectrum and its effects. Source: www.rroij.com*

### 2.1.5 Dose Limits

The International Basic Safety Standards for Protection against Ionizing Radiation and for the Safety of Radiation Sources (BSS) was built by the International Commission on Radiological Protection (ICRP) provides a worldwide basis for harmonized radiation protection standards. The recommendation for the occupational exposure of radiation worker should be controlled, and the limits should not be exceeded an effective dose of 20 mSv per year average over 5 consecutive years. Moreover, the effective dose for public exposure shall not exceed the following limits of 1 mSv in a year and in special circumstances, an effective dose is up to 5 mSv in a single year provided that the average dose over 5 years does not exceed 1 mSv per year. In case of emergency exposure situations, all workers undertaking intervention shall be kept the effective dose below twice the maximum single year the dose limit except for the saving life action, in which all effective dose should be kept below ten times the maximum single year dose limit. If the radiation doses are very high, the effect on the body will appear very soon after the exposure. Even the dose is not high enough to cause serious injury, it is still harmful to the health. So the radiation workers should follow the concept of Radiation Protection ALARA (As Low As Reasonably

Achievable) in order to avoid the unnecessary exposure of workers to ionizing radiation. [23], [24]

2.1.6 Dosimetry

Exposure (X) is used to measure the gamma rays ionizing's ability. It is a quantity expressing the amount of ionization caused in air by X- or gamma radiation. In SI unit of ionizing of radiation exposure, coulomb per kilogram (C/kg) and the roentgen (R) is an obsolete traditional unit of exposure and roentgen per hour (R/hr) was the unit of exposure rate. At the standard condition of 0 $^0$C, 760 mmHg, the amount of radiation in 1 R was equaled to the amount of radiation required to produce 1 electrostatic unit of charge (1 esu) in air 0.001293 g (in 1 cm$^3$ of air).

We have 1 X-unit = 1 C/kg

And 1 R = 1 esu / 0.001293 g

But, 1 ion pair = $4.80 \times 10^{-10}$ esu = $1.60 \times 10^{-19}$ C

Then 1 C = $3.00 \times 10^{9}$ esu

So, 1 R = $2.58 \times 10^{-4}$ C/kg or 1 X-unit = 1 C/kg = 3881 R (1)

However, the effect of gamma and other ionizing radiation on living tissue is more closely related to the amount of energy deposited rather than the charge. This is called the absorbed dose (D). In SI unit of absorbed dose, Gray (Gy) and absorbed dose rate, Gray per hour (Gy/hr), and is defined as an energy deposition of 1J/kg. The rad is the deprecated CGS unit, equal to 0.01 J deposited per kg. So, 100 rad = 1 Gy.

We have 1 X-unit = 1 C/kg

Which, 1 ion pair = $1.60 \times 10^{-19}$ C needs 34 eV in air

And 1 eV = $1.60 \times 10^{-19}$ J

So, 1 X-unit = 34 J/kg = 34 Gy (1 J/kg = 1 Gy) (2)

When (1) = (2)

3881 R = 34 Gy then 1 Gy = 114 R (3)

Moreover, the equivalent dose (H) is used to measure the biological effect of radiation on human tissue and it is equivalent to absorbed dose in gamma radiation. We use Sievert (Sv) is the SI unit of equivalent dose and rem is the deprecated CGS unit of equivalent dose then we get 1 Sv = 100 rem. Therefore, the units of equivalent dose rate were Sievert per hour (Sv/hr) and rem per hour (rem/hr).

As follow the equation: $H\ (Sv) = D\ (Gy) \times Q$

Which, D (Gy) is absorbed dose

And Q is quality factor (for all the energies of gamma rays, Q = 1)

So, $H\ (Sv) = D\ (Gy)$

Based on (3), 1 Gy = 114 R then 1 Sv = 114 R

Or 1 Gy/hr = 1 Sv/hr = 114 R/hr [9], [10]

## 2.2 Detectors

Radiation detectors have been divided into three categories based on the characteristic of the detector materials and the radiation interactions with the detector to produce the measure events. [25], [26]



### 2.2.1 Gas-filled Detectors

The radiation interact with the filling gas, producing ion-pairs which are collected by charge electrons. They are categorized as Geiger Muller counter, Proportional counter, and Ionization Chamber counter. Several gas-filled detectors are based on the effects produced when charge particles pass through a gas. These types of radiation detector contain of two electrodes to which a bias potential is applied for charge collection process.

Geiger Muller Counter: this counter is operated only pulse mode. The output signal is independent of the primary ionization because of its gas multiplication factor is extremely high. This counter is designed in many styles such as pancake GM, side window, end window, and anticoincident guard detector for low background counter.

These various types of Geiger Muller counters have been used in many special applications to detect radiation such as activity measurement, survey meter, gamma monitor, and pocket dosimetry.

Proportional Counter: this type of counter is almost always operated in pulse mode and rely on the phenomenon of gas multiplication to amplify the charge represented by the original ion-pairs created within the gas. An average gas multiplication factor is given by M = total number of electrons divide by one ion-pair created by incident radiation. There are many styles of proportional counter such as gas-filled counter, gas-flowed counter, gas-recharged counter, photon recoil counter, and $BF_3$ & $^3He$ proportional counter. All types of proportional counter have been used in many special applications such as surface contamination, XRF, XRD, $2\pi$ and $4\pi$ counter, environmental application, neutron monitor, and neutron dosimeter.

Ionization Chamber Counter: the typical ionization currents in most application are extremely small ($<10^{-12}$ A), and the leakage current between anode and cathode must be blocked by guard ring. There are two types of ionization chamber one is free air chamber and another is Argon pressurized chamber. Ionization chamber is used in some special application such as dosimeter and dose calibration.

### 2.2.2 Scintillation Detector



This type of detector is composed of two parts scintillator coupled with photosensitive.

Scintillators are photo luminescent materials that absorb energy from radiations, high energy particle, gamma radiation and x-rays, and fluoresce with the wavelength of light that is easily detected. Its properties can be found in both organic and inorganic materials.

Organic Scintillator: the materials that are efficient organic scintillators belong to the class of aromatic compounds. They consist of planar molecules made up of benzenoid rings. The production of light emission in organic scintillators is the result of molecule transition. They also are readily adaptable to the detection of fast neutron or photon by the addition of some suitable materials into scintillator.

Inorganic Scintillator: most of inorganic scintillators are crystals of alkali metals, in particular alkali halide, which is activated with a small concentration of impurity. There are many types of inorganic scintillators such as NaI(Tl), CsI(Tl), CsI(Na), LiI(Eu) and $CaF_2$(Eu). The luminescence of inorganic scintillators can be generated by radiation induced excitation pair and de-excitation of excited electron in electronic energy states of atom. The light emitted by a scintillator is primarily the result of transitions of the activator atoms.

### 2.2.3 Semiconductor detector

Semiconductor detector is solid state device that operate similar to gas ionization chamber, but the charge carriers in semiconductors are electrons and holes. They are most commonly used when the best energy resolution is intended. In a metal, the highest occupied energy band is not completely full and electrons can easily migrate. The most semiconductors are made from silicon (Si) and germanium (Ge). Also, some compounds semiconductors such as CdTe, CdZnTe, $HgI_2$ can also be made. The important advantage of these detectors is their superior energy resolution.

## 2.3 Complementary Metal Oxide Semiconductor (CMOS) Image Sensors

Complementary Metal Oxide Semiconductor (CMOS) is a type of silicon semiconductor that has been found in many electrical devices. CMOS sensors technologies have been developed since 1970s, but they had unacceptable performance. Until 1990s, first CMOS designs were yielding chips with smaller pixel size, noise reduction, more capable image processing algorithms and larger image array. Nowadays, imaging technologies mainly improving CMOS imaging performance, functional capability and their flexibility. CMOS image sensor is a device in camera that has ability to convert the optical image presented by the lens into the electrical signal. They are mixed-signal circuits containing pixels, analog signal processors, analog-to-digital converters, bias generators, timing generators, digital logic and memory. Metal Oxide Semiconductor is a reference to the physical structure of certain field-effect transistors, having a metal gate electrode placed on top of an oxide insulator, which in turn is on top of semiconductor material (Poly silicon). Their architecture can be divided into four main blocks: 1). Pixel Array or Pixel Circuits are mainly divided into two parts such as Passive Pixels (PPS) which are the first CMOS imagers that based on photodiodes without internal amplification and Active Pixels (APS) are sensors that implement buffer per pixel (this buffer is a simple source follower). 2). Analog Signal Processing: improving the performance and functionality of CMOS image sensors. 3). Row and Column selector (readout methods): they have an important influence in the sensor performance. It is suitable for ultra-high sensitivity and radiation imaging systems. And 4). Timing and control: high speed imaging and control the noises.

The CMOS sensor performances use large arrays of Photosite or it is called pixel. The basic steps of CMOS sensor are focused on five points: 1). the light (input) that is determined by the structure (material and geometry): the light is directed from the camera lens converted into electrons. 2). Charge Accumulation: more light enter, more electron come into semiconductor "bucket". 3). Transfer: signal must move out from the photo sensitive area of the chips. 4). Charge to voltage conversion: the accumulated charge must be converted as a voltage signal. And 5). Amplification: to make the charge-to-voltage conversion is much stronger than before it handed off to the camera circuitry.

A major advantage that CMOS image sensors enjoy over other sensors is the ability to integrate a number of processing and control functions, which lie beyond the primary task of photon collection, directly onto the sensor integrated circuit. These features generally include timing logic, exposure control, analog-to-digital conversion, shuttering, white balance, gain adjustment, and initial image processing algorithms. In order to perform all of these functions, the CMOS integrated circuit architecture more closely resembles that of a random-access memory cell rather than a simple photodiode array. [27], [28]

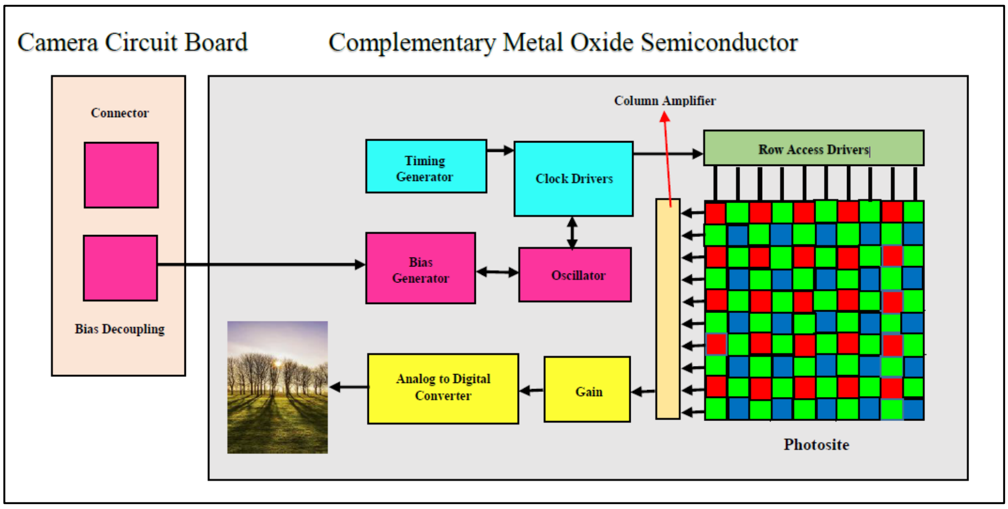


*Figure 7. The diagram of CMOS image sensor inside the camera*

## 2.4 Gamma rays interact with CMOS Image Sensors

Ionization damage is the dominant mechanism when energetic photons (gamma and x-rays) interact with the solid-state matter. The damage causes charge-trapping at Si-$SiO_2$ interfaces and trap build-up at these locations. When a broad wavelength band of gamma radiation is incident on specially doped silicon semiconductor materials, a variable number of electrons are released in proportion to the photon flux density incident on the surface of a photodiode. In effect, the number of electron produced is a function of the wavelength and the intensity of radiation striking the semiconductor. Electrons are collected in a potential well until the integration (illumination) period is finished, and then they are either converted into a voltage. The measure voltage is then pass through and analog-to-digital converter, which form a digital electronic representation of the scene imaged by the sensor. There are three different ways that ionizing rays can interact with the atom under consideration. In Photoelectric effect, when ionizing radiations pass through a semiconductor material, the energetic photons ionize the target atom and generate electron-hole pairs. The photon is completely absorbed in this process. Also, Compton scattering effect the incoming ionizing radiation is scattered on interacting with the atom, just like visible light is diffused from a rough surface. And Pair Production, the incident photon is completely annihilated. This phenomenon occurs for higher energy photons.

All in all, whether gamma rays interact with the CMOS circuit in term of the photoelectric effect, Compton scattering effect or pair production, the end result will be the production of electrons and positive ions. The gamma rays continually produce ionized electrons then when there is an electric field present, the electrons will be collected. However, they will recombine with hole during the period between each image collection. [29], [30]

## 2.5 Calibration of Radiation Monitoring Instruments

In accordance with ICRP publication, usually the upper limits to organ doses rather than actual values are assessed when the reading of dosimeters are recorded. Nevertheless, it has become conventional to note and record all radiation doses about the detection threshold of the personal dosimeter.

There are basically two techniques for calibrating radiation instruments. These are the uses of radiation fields whose properties are well known, and the use of less well-defined radiation fields where the calibration is by the substitution technique. In the first technique the radiation field can be defined from a knowledge of certain parameters of a standard source or by measurements made with a secondary standard. Certain factors, such as a large amount of scattered radiation, can make reliable specification of radiation field difficult and in these cases the calibration is best made by the substitution technique. [31]

In calibration work, by using Inverse Square Law for point source, we can follow this equation below to calculate exposure rate:

$$\text{Exposure rate} = \Gamma \times \frac{A}{d^2} \quad \text{which,}$$

Exposure rate (R/hr)

Γ: specific gamma ray constant ($R.m^2$/ Ci.hr)

A: current activity (Ci)

d: distance (m)

In this table is shown about Gamma-ray sources suitable for calibration to use in laboratory or research center:

*Table 1. Gamma rays sources suitable for calibration*

| Radionuclides | Effective quantum energy (keV) | Half-life | Specific gamma ray constant (R.m$^2$/Ci.hr |
|---|---|---|---|
| $^{125}$I | 35.0 | 59.2 days | 0.070 |
| $^{241}$Am | 60.0 | 458 years | 0.013 |
| $^{192}$Ir | 300-600 | 74..3 days | 0.440 |
| $^{137}$Cs | 662 | 29.9 years | 0.323 |
| $^{60}$Co | 1250 | 5.23 years | 1.30 |
| $^{226}$Ra | 180-2200 | 1608 years | 0.825 |

# Chapter 3

# MATERIALS AND METHODOLOGY

## 3.1 Materials

### 3.1.1 Smartphones

In this work, the four models of smartphones were chosen for doing experiment.

#### 3.1.1.1 Samsung Galaxy GT-S5570 mini

*Table 2. The specifications of Samsung Galaxy GT-S5570 mini (www.gsmarena.com/ Samsung_galaxy_mini_s5570-3725.php, visited page: 01st September 2015)*

| Specifications | |
|---|---|
| Platform | Camera |
| OS: Android OS, version 2.2, upgradable to version 2.3 | Primary: 3.15 MP, 2048×1536 pixels, with Back-Side Illuminated CMOS sensor |
| Chipset: Qualcomm MSM7227 snapdragon S1 | Features: Geo-tagging |
| CPU: 600 MHz ARM version 6 | Video: 320p, 15 frames per second |
| GPU: Adreno 200 | Secondary: No<br>Aperture: No |


*Figure 8. Samsung Galaxy GT-S5570 mini.*

3.1.1.2 Samsung Galaxy SII GT-I9100

*Table 3. The specifications of Samsung Galaxy SII (www.gsmarena.com/ Samsung_galaxy_i9100_galaxy_s_ii-3621.php, visited page: 01st September 2015)*

| Specifications | |
|---|---|
| Platform | Camera |
| OS: Android OS, version 2.3.4, upgradable to version 4.0.4, and version 4.1 | Primary: 8 MP, 3264×2448 pixels, LED flash, with Back-Side Illuminated CMOS sensor |
| Chipset: Exynos 4210 | Features: Geo-tagging, touch focus, face/smile detection |
| CPU: Dual-core 1.2 GHz Cortex-A9 | Video: 1080p, 24 frames per second, full HD video recording |
| GPU: Mali-400 | Secondary: 2 MP<br>Aperture: f/2.7 |


*Figure 9. Samsung Galaxy SII*

3.1.1.3 Samsung Galaxy SIII GT-I9300

*Table 4. The specifications of Samsung Galaxy SIII (www.gsmarena.com/ Samsung_galaxy_i9300_galaxy_s_iii-4238.php, visited page: 01st September 2015)*

| Specifications | |
|---|---|
| Platform | Camera |
| OS: Android OS, version 4.0.4, upgradable to version 4.3 | Primary: 8 MP, 3264×2448 pixels, LED flash, with Back-Side Illuminated CMOS sensor |
| Chipset: Exynos 4412 Quad | Features: Geo-tagging, auto focus, touch focus, face/smile detection |
| CPU: Quad-core 1.46 GHz Cortex-A9 | Video: 1080p, 30 frames per second, full HD video recording |
| GPU: Mali-400 MP4 | Secondary: 1.9 MP, 720p, 30 frames per second |
| | Aperture: f/2.6 |


*Figure 10. Samsung Galaxy SIII*

3.1.1.4 Huawei Ascend P7

*Table 5. The specifications of Huawei Ascend P7 (www.gsmarena.com/huawei_ascend_p7-6124.php, visited page: 01st September 2015)*

| Specifications | |
|---|---|
| Platform | Camera |
| OS: Android OS, version 4.4.2 | Primary: 13 MP, 4160×3120 pixels, LED flash, with AF Back-Side Illuminated CMOS sensor |
| Chipset: Hisilicon kirin 910T | Features: Geo-tagging, auto focus, touch focus, face/smile detection, panorama, HDR |
| CPU: Quad-core 1.8 GHz Cortex-A9 | Video: 1080p, 30 frames per second, full HD video recording |
| GPU: Mali-450 MP4 | Secondary: 8 MP, 1080p, 30 frames per second, full HD video recording |
| | Aperture: f/2.0 |


*Figure 11. Huawei Ascend P7*

### 3.1.2 Detectors

3.1.2.1 The Hand-held Gamma and Neutron Search Instrument HDS-101 GN at the Department of Nuclear Engineering, Chulalongkorn University

The Hand-held Gamma and Neutron Search Instrument HDS-101 GN is an ultra-sensitive gamma/neutron radiation alarming detector (More detail about the specification see appendix A). In this study, this hand-held detector was used to measure the equivalent dose rate of gamma rays from $^{192}$Ir at the Department of Nuclear Engineering.


*Figure 12. Hand-held gamma and neutron detector HDS-101 GN*

3.1.2.2 2575 600cc Thin Window Ionization Chamber and Electrometer “DOSE1” at the Department of Medical Sciences (DMSc)

This 2575 600cc thin window ionization chamber is designed as a high performance chamber for the measurement of exposure to x and gamma rays. In Secondary Standard Dosimetry Laboratory (SSDL), it was used to measure the exposure rate of gamma rays from $^{137}Cs$ and $^{60}Co$.

*Figure 13. 2575 600cc thin window Ionization Chamber*

Electrometer “DOSE1” is a portable, single channel, high-precision reference class electrometer that is used with ionization chamber of absorbed dose. In this study, this electrometer was used with 2575 600cc thin window ionization chamber to measure the exposure rate of gamma radiation.

*Figure 14. Electrometer "DOSE1"*

3.1.2.3 Hand-held Survey Meter Model Inspector and Ionization Chamber Type A6 REF 92716 at the Office of Atoms for Peace (OAP)

This radiation inspector is a kind of hand-held survey meter, which is used to measure the dose rate of gamma radiation. In this study, we used this detector to measure the gamma ray exposure rate from $^{137}Cs$ in SSDL. This inspector was provided by the SSDL.


*Figure 15. Radiation inspector*

This ionization chamber type A6 REF 92716 is designed for the measurement of exposure to x and gamma rays. (The calibration certificate can see in appendix B). In SSDL, it was used to measure the gamma rays from $^{137}Cs$ and $^{60}Co$.

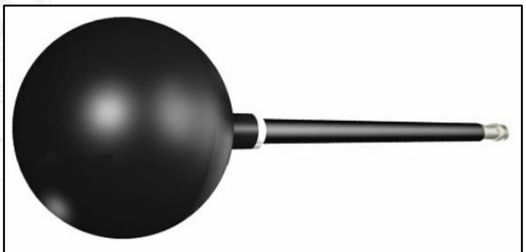

*Figure 16. Ionization Chamber type A6 REF 92716*

### 3.1.3 Gamma Ray Sources

#### 3.1.3.1 $^{192}$Ir Radiography Gamma Ray Projector from NDT, Thailand

This $^{192}$Ir was used to investigate the sensitivity of smartphones (Samsung Galaxy GT-S5570 mini, Samsung Galaxy SII, Samsung Galaxy SIII and Huawei Ascend P7) at the Department of Nuclear Engineering, Chulalongkorn University.

*Table 6. The properties of $^{192}$Ir radiography gamma ray projector from NDT, Thailand*

| Properties | |
|---|---|
| Radionuclide | Ir-192 |
| Half-life | 74.3 days |
| Effective Quantum Energy (keV) | 300-600 |
| Specific Gamma ray Constant ($R.m^2/Ci.hr$) | 0.440 |
| Source Activity | On 21st October 2014, A=12.44 Ci |
| Shielded container | Depleted uranium |

*Figure 18. The $^{192}$Ir source in the shielded container from NDT, Thailand*

*Figure 17. Wind-out which was used to bring the $^{192}$Ir from the shielded container*

3.1.3.2 $^{137}$Cs Dose Rate Calibration Sources

Both of these $^{137}$Cs sources were used for investigation of sensitivity of smartphones (Samsung Galaxy SII, Samsung Galaxy SIII and Huawei Ascend P7) and calibration of smartphones (Samsung galaxy SIII and Huawei Ascend P7) at the DMSc and OAP.

*Figure 19. The $^{137}$Cs source in the DMSc*


*Figure 20. The $^{137}$Cs source in the OAP*

*Table 7. The properties of $^{137}$Cs source in the SSDL*

| Properties | |
|---|---|
| Radionuclide | Cs-137 |
| Half-life | 29.9 years |
| Effective Quantum Energy (keV) | 662 |
| Specific Gamma ray Constant ($R.m^2/Ci.hr$) | 0.323 |
| Exposure Rate | Exposure rates were provided by the SSDL of the DMSc and the OAP |
| Shielded container | Lead Shielding |

3.1.3.3 $^{60}$Co Dose Rate Calibration Sources

Both of these $^{60}$Co sources were used for investigation sensitivity of smartphones (Samsung Galaxy SII, Samsung Galaxy SIII and Huawei Ascend P7) in SSDL of the DMSc and OAP.

*Figure 21. The $^{60}$Co source at the DMSc*

*Figure 22. The $^{60}$Co Source at the OAP*

*Table 8. The properties of $^{60}$Co in the SSDL*

| Properties | |
|---|---|
| Radionuclide | Co-60 |
| Half-life | 5.23 years |
| Effective Quantum Energy (keV) | 1250 |
| Specific Gamma ray Constant ($R.m^2/Ci.hr$) | 1.30 |
| Exposure Rate | Exposure rates were provided by SSDL at the DMSc and the OAP |
| Shielded container | Lead Shielding |

### 3.1.4 Software Programme

#### 3.1.4.1 AOAO Video to Picture Converter Software

AOAO Video to Picture Converter software version 4.0 was established in 2008, consistently dedicated to satisfy users with diversified consumer software products and services.

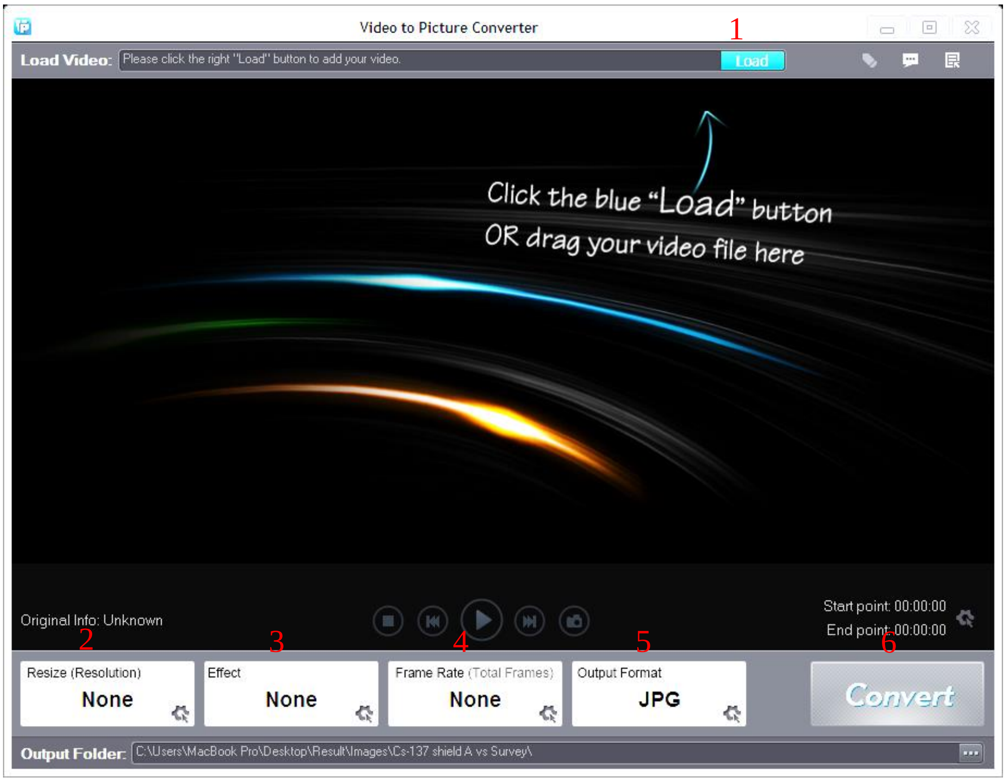


*Figure 23. The platform of AOAO Video to Picture Converter software*

1. Loading Video into software
2. Resize the resolution of each converted pictures
3. Set the type of effect of each converted pictures
4. Set the output format of converted picture
5. Set the amount of frame rate based on the properties of video
6. Convert the video to picture

3.1.4.2 ImageJ Software

The ImageJ 1.46r was established in 2012. It is a public domain Java image processing and analysis program inspired by NIH Image for the Macintosh. This program can display, edit, analyze, process, save, and print 8-bit, 16-bit and 32-bit images. Also, it can read many formats including TIFF, GIF, JPEG, BMP, DICOM, FITS and raw. Downloading the software is free and available for Windows, Mac OS and Linux (http://imagej.nih.gov/ij/download.html), and details on how to install ImageJ are available at http://imagej.nih.gov/ij/docs/install/. [32]

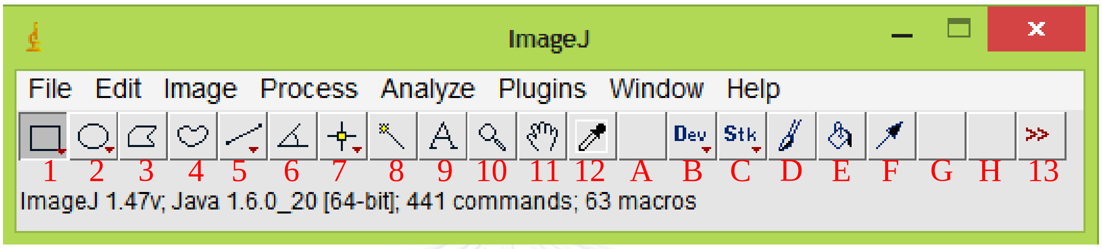


*Figure 24. The platform of ImageJ software*

In the menu bar of ImageJ, it is organized in eight menus such as:

File Mode: basic file operations (opening new images).

Edit Mode: editing and drawing operations as well as global settings.

Image Mode: conversion and modification of images including geometric transformations.

Process Mode: image processing, including point operations, filters and arithmetic operations.

Analyze Mode: statistical measurements, profile and histogram plotting and other operation related to image analysis.

Plugins Mode: commands for creating, editing and managing add-ons, listing all the user-installed Macros, Scripts and Plugins installed in the ImageJ/Plugins/dictionary.

Window Mode: selection and management of open Windows.

Help Mode: updates, documentation resources and version information.

Also, the ImageJ toolbar contains tools for making selections, drawings, zooming and scrolling, etc.

1. Rectangular Selection Tool and Rounded Rectangular Selection Tool
2. Oval Selection Tool, Elliptical Selection Tool and Brush Selection Tool
3. Polygon Selection Tool
4. Freehand Selection Tool
5. Straight Line Selection Tool, Segmented Line Selection Tool, Freehand Line Selection Tool and Arrow Tool
6. Angle Tool
7. Point Tool and Multi-point Tool
8. Wand Tool
9. Text Tool
10. Magnifying Glass
11. Scrolling Tool
12. Color Picker Tool
13. More Tools Menu

A-H Customized tool

## 3.2 Methodology

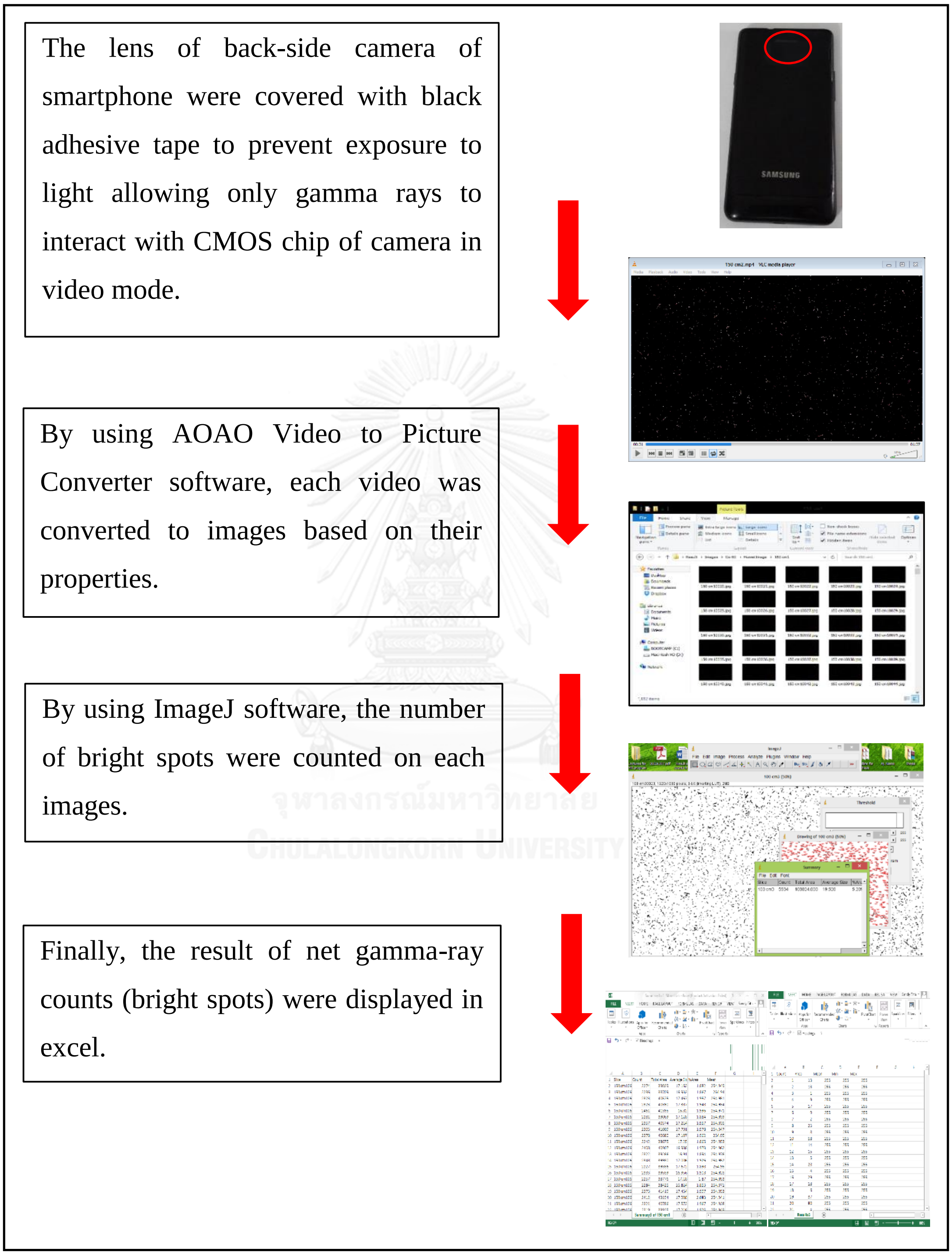


*Figure 25. The summary of method to detect gamma radiation*

### 3.2.1 Experimental Procedures

#### 3.2.1.1 Smartphones Preparation

In this study, the back-side camera of each smartphone was used. During the experiment, the phones were set in video mode while the camera lenses were cover with black adhesive tape. The preparation was shown in the pictures below:


*Figure26. The back-side camera of smartphone*


*Figure27. The back-side camera which covered by the adhesive tape*

*Figure 26. The video processing of smartphone*

In video mode, the highest resolution mode of recorded video was chosen base on the properties of each smartphones such as:

For Samsung Galaxy GT-S5570 mini, the recorded video was set the maximum resolution as 320 × 240 pixels and frame rate was 15 frames per second.

For Samsung Galaxy SII, the recorded video was set the maximum resolution as 1920 × 1080 pixels full HD video and frame rate was 24 frames per second.

For Samsung Galaxy SIII, the recorded video was set the maximum resolution as 1920 × 1080 pixels full HD video and frame rate was 30 frames per second.

And Huawei Ascend P7, the recorded video was set the maximum resolution as 1920 × 1080 pixels full HD video and frame rate was 30 frames per second.

3.2.1.2 Investigation the Sensitivities of Smartphones by Using $^{192}$Ir Radiography Gamma Ray Projector

To investigate the sensitivity of each smartphones to gamma radiation, $^{192}$Ir was used in this experiment at the Department of Nuclear Engineering, Chulalongkorn University. The experiment was done on 23$^{rd}$ January 2015, 19$^{th}$ February 2015 and 10$^{th}$ March 2015 by using these four models of phone, Samsung Galaxy GT-S5570 mini, Samsung Galaxy SII, Samsung Galaxy SIII and Huawei Ascend P7.

We used wind-out to bring the $^{192}$Ir source to the edge of projection tube, which this projection tube was put inside the closed-door room and processed the video mode to record the bright spots of gamma rays interact with CMOS chip.

*Figure 27. The use of wind-out to bring $^{192}$Ir from the shielded container to the edge of projection tube*

*Figure 29. $^{192}$Ir source in the shielded container*

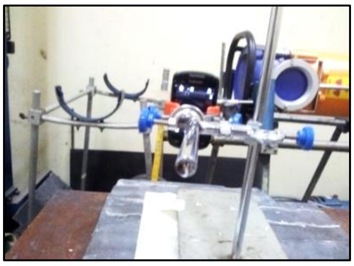

*Figure 28. Video capturing*



3.2.1.3 Investigation the Sensitivities of Smartphones by Using $^{137}$Cs Calibration Sources

After the result from the investigation of sensitivity of each smartphone with $^{192}$Ir, we found that Samsung Galaxy GT-S5570 mini given the result of low counts of gamma rays, so with $^{137}$Cs, there were only three models of smartphone that were used. The experiment were done in SSDLs of the DMSc and OAP.

At the DMSc, three models of smartphone, Samsung Galaxy SII, Samsung Galaxy SIII and Huawei Ascend P7 were calibrated on 11$^{th}$ June 2015. The standard values of exposure rate were provided by the SSDL. By using the control unit for $^{137}$Cs irradiation system, we could controlled the $^{137}Cs$ source's moving. Moreover, it had a counting time function, that we could limit the time exposure for gamma rays.


*Figure 30. The control unit for $^{137}Cs$ irradiation system*

*Figure 31. $^{137}Cs$ source in lead shielding at the DMSc*

On the other hand, the experiment that was done at the OAP was to calibrate the selected smartphones (Samsung Galaxy SIII and Huawei Ascend P7) after we got the result of count from the experiment at the DMSc. At the OAP, the experiment of calibration was done on 28th July 2015. Furthermore, on 03rd September 2015 we had done another experiment to compare the result of dose rate from our smartphone (Huawei Ascend P7) with standard values and survey meter. The standard values of exposure rate were provided by SSDL.


*Figure 32. The control unit for $^{137}Cs$ source*

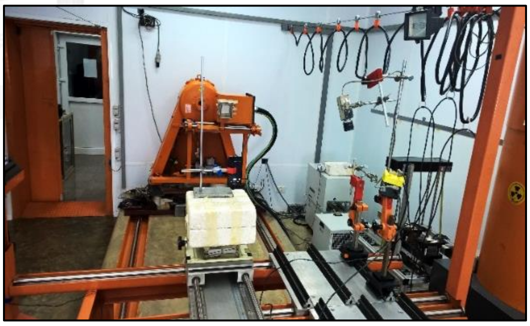

*Figure 33. $^{137}Cs$ source in lead shielding at the OAP*

3.2.1.4 Investigation the Sensitivities of Smartphones by Using $^{60}$Co Calibration Sources

$^{60}$Co was used to investigate the sensitivity of each smartphones (three models of smartphones as same as in $^{137}$Cs). The experiment were done in the SSDL of the DMSc and OAP.

At the DMSc, the three models of smartphone, Samsung Galaxy SII, Samsung Galaxy SIII and Huawei Ascend P7 were calibrated on 09$^{th}$ June 2015 with the high dose rate of $^{60}$Co. The standard values of exposure rate were provided by the SSDL.


*Figure 34. The control unit for $^{60}$Co source*

*Figure 35. $^{60}$Co source in teletherapy machine at the DMSc*

At the DMSc, the exposure rate of $^{60}$Co was very high, so we calibrated smartphones with the low exposure rate $^{60}$Co at the OAP too. On 03$^{rd}$ August 2015 we did the experiment with low dose rate of $^{60}$Co in SSDL and the standard values of exposure rate were provided by that facility.

*Figure 36. The control unit of $^{60}$Co source*

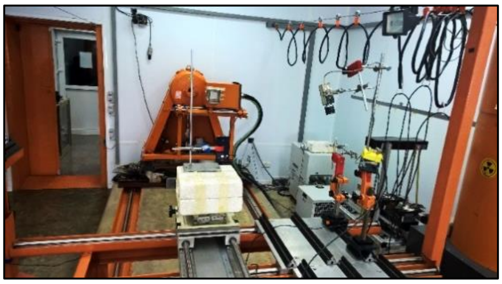

*Figure 37. $^{60}$Co source at the OAP*

### 3.2.2 Software Programme Procedure

#### 3.2.2.1 AOAO Video to Picture Converter Software

By using AOAO Video to Picture Converter software, all of the videos were converted to pictures based on their properties.

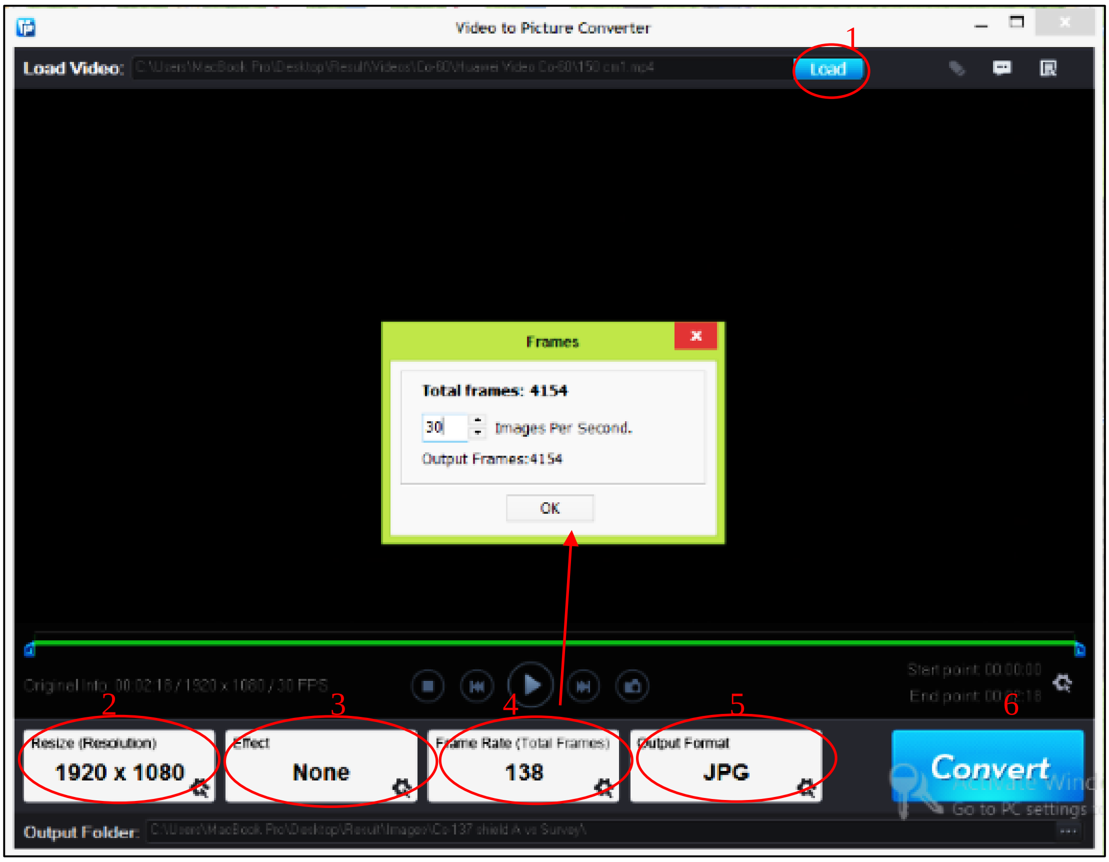


*Figure 38. The Processing of converting video to pictures by using AOAO video to picture converter software*

The procedure was followed as the steps below:

1. Loading the Video: by clicking the blue "Load" button, we could drag the video into this software, and the video was still kept as original.
2. Resize (Resolution): in this step, we can resize the resolution of the video. However, in our case we would keep all the original resolution, like the videos from Samsung Galaxy GT-S5570 mini were recorded as size 320 × 240 pixels, the videos from Samsung Galaxy SII were recorded as size 1920

×1080 pixels, the videos from Samsung Galaxy SIII were recorded as size 1920 ×1080 pixels, and the videos from Huawei Ascend P7 were also recorded as size 1920 ×1080 pixels as well.

3. Effect Mode: in this mode, we did not change anything from the original video.
4. In the step, frame rate were changed based on the property of the original video. For the video of Samsung Galaxy GT-S5570 mini, the frame rate was chosen as 15 frames per one second. With the video of Samsung Galaxy SII, the frame rate was 24 frames per one second. And both of Samsung Galaxy SIII and Huawei Ascend P7, the frame rate was set as 30 frames per second.
5. For Output Format Mode, all the images were converted and saved as ".JPG".
6. Finally, we could convert the video to pictures successfully. And each images were shown as the figure below.

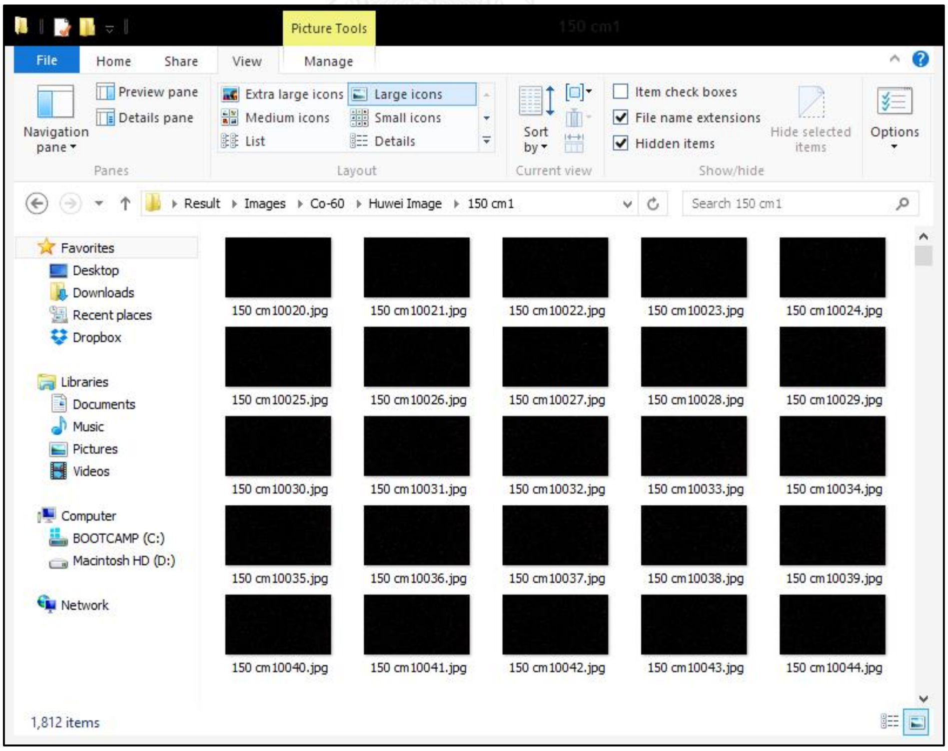


*Figure 39. The folder of images after converting by using AOAO video to Picture Converter software*

3.2.2.2 ImageJ Software

In this study, the four menus were used such as File mode, Edit mode, Image mode and Analyze mode.

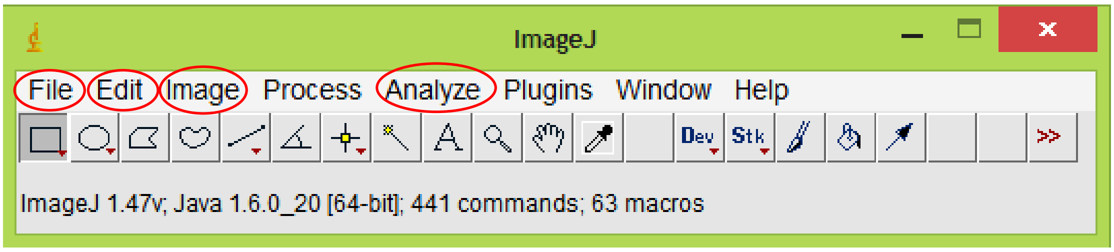


*Figure 40. The menus of ImageJ software that used in this process*

*3.2.2.2.1 File Mode*

In this mode, by selecting the submenu of "Import" and choose Image Sequence to open a series of images in a chosen folder as a stack.

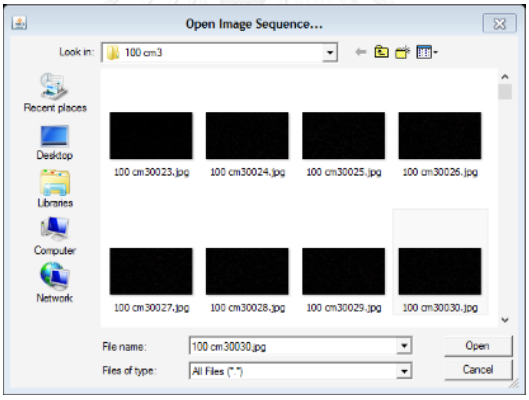


*Figure 41. Image folder*

Number of images: specifies how many images to open

Starting images: if set to n, import will start with n$^{th}$ image in the folder

Increment: one of a series of increases

Scale images: is a value of memory requirement

File name contains: not necessary to put the name when we choose the Sort names numerically

And by clicking OK mean all the option fillings are completed

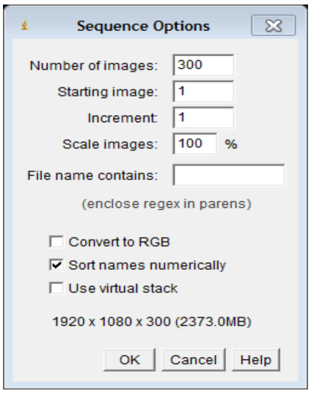


*Figure 42. Submenu "Sequence Options" in ImageJ*

*3.2.2.2.2 Edit Mode*

In this mode, the submenu of "Inverse" was selected to create a reversed image, similar to a photographic negative, of the entire image or selection.

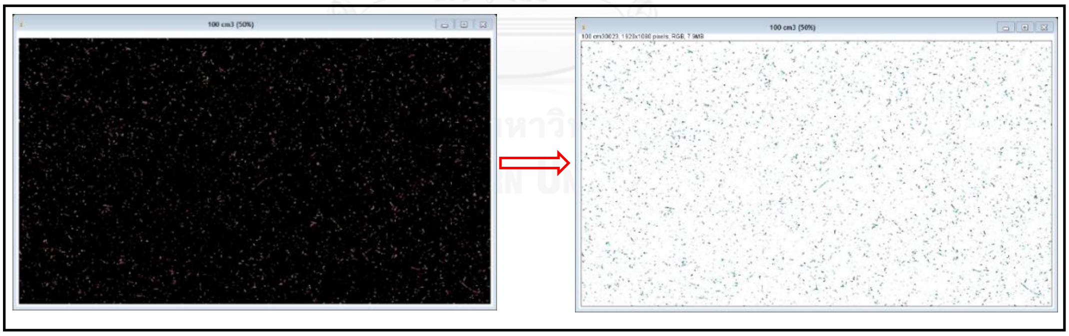

*Figure 43. The inversing of image*

*3.2.2.2.3 Image Mode*

In this mode, the submenu of "Type" was used to determine the type of the active image or to convert it to another type. In this study, we chose "8-bit" type to convert the image to 8-bit grayscale by linearly scaling from min-max to 0-255. And another submenu in this mode was "Adjust", and we used this submenu to set the threshold level.

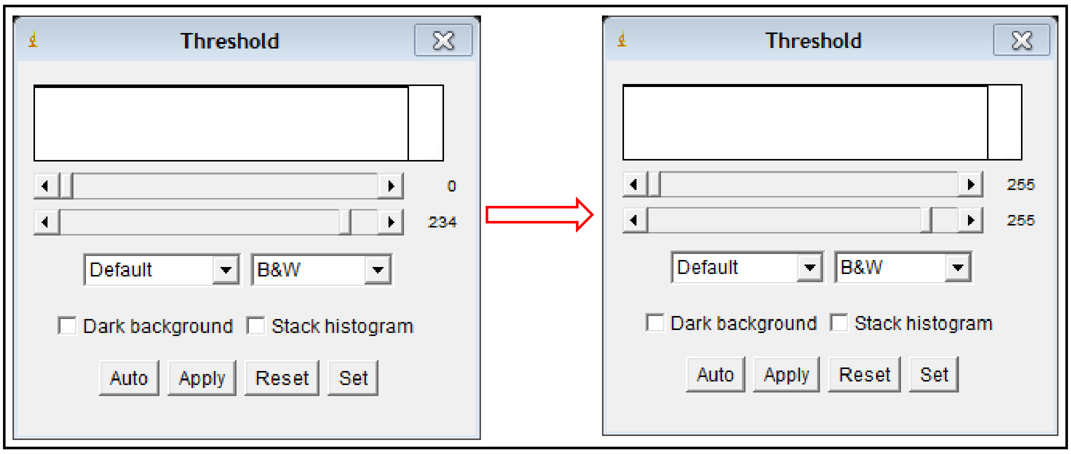


*Figure 44. Setting the threshold and applying to get the total threshold*

In our work with gamma radiation, the threshold of each smartphones were set in zero background. It was meant that before counting the image sample, the amount of standard pictures were succeeded without radiation exposure and we could determine the threshold. Finally, the result of counts on the sample images were the number of net gamma-ray counts.

*3.2.2.2.4 Analyze Mode*

In this mode, the submenu of "Analyze particles" was selected to count and measure object in threshold images.

Size (pixel$^2$): by setting from 0-infinity, means that all the particles on the image scale are counted.

Circularity: by setting from 0.00-1.00, means that all the particles with perfect circle are counted.

Show: this drop-down menu specifies which image that ImageJ should display after analysis.

So, we chose to display results, summarize, exclude on edges, and include holes then by clicking OK to get the result.

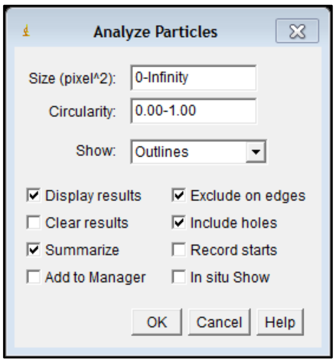


*Figure 45. The process of particles analyzing*

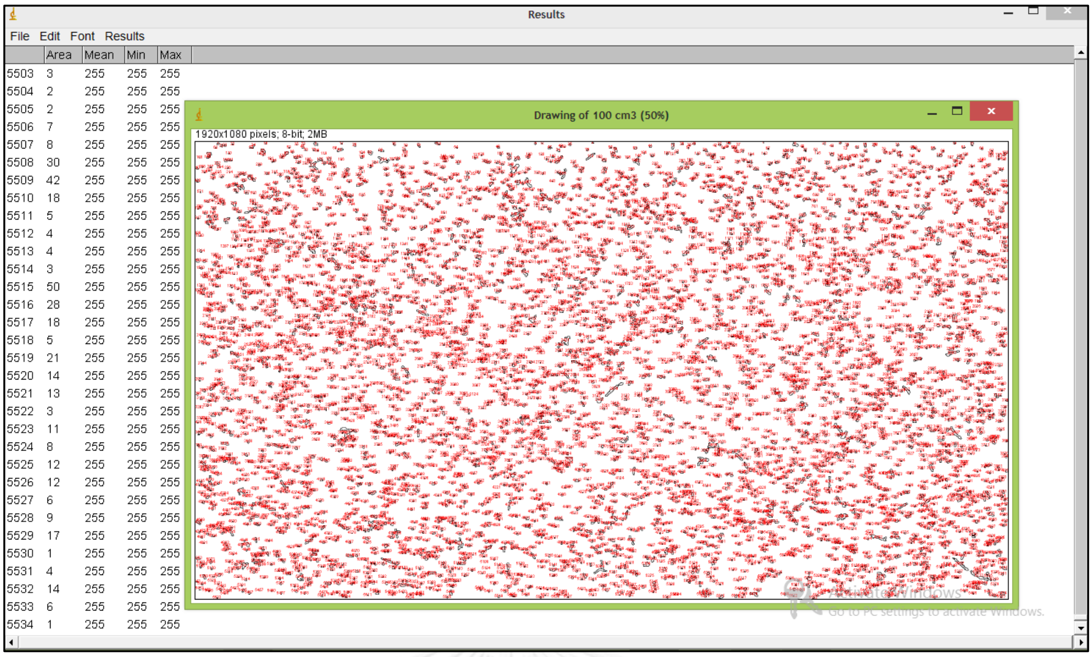


*Figure 46. The number of gamma-ray bright spots by using ImageJ software*

By getting the result from ImageJ analysis, finally we could use all these results to compare with the equivalent dose rate.

3.2.2.3 In-house Android Application Software

This Android application software was developed for real-time counting of the bright spots on the image.

Select Video: by choosing “Real Time” mode

Set Size: Setting the max and min of area

Set Threshold: Setting number of threshold to get the max counts

Set Duration: set the duration for using this software

Set Offset: not necessary for real-time counting

Watch History: see the result recording

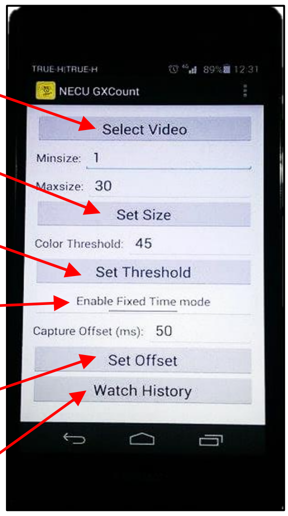


*Figure 47. Platform of Real-time counting software*

After the counts of bright spots were obtained from this real time counting software, another function of the software is to determine the dose rate.



Set Formula: by using the equation from the real-time counting, which x is the number of count and y is dose rate.

Set Duration for Dose Rate: how long to determine dose rate per one time

Set Iteration: to set how many iteration to get the average

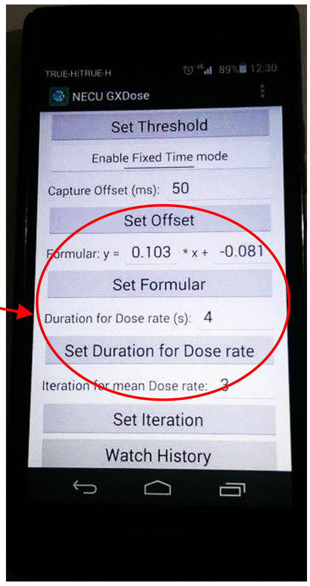


*Figure 48. More functions to determine dose rate*

# Chapter 4

# RESULTS AND DISCUSSION

All the results have been described by the graph of the count rate (count per second) plotted against the dose rate (milisievert per hour, mSv/hr) from each smartphone for gamma rays from $^{192}$Ir, $^{60}$Co and $^{137}$Cs sources.

## 4.1 Response of Smartphones for $^{192}$Ir

The exposure rates of $^{192}$Ir were calculated by using Inversed Square Law for point source. The calculation was shown in appendix D, and the conversion of exposure rates of $^{192}$Ir to equivalent dose rates were shown in appendix D too.

*Table 9. Comparison the sensitivity of all smartphones by using $^{192}$Ir*

| Equivalent Dose Rate (mSv/hr) | Samsung Galaxy GT-S5570 (cps) | Samsung Galaxy SII (cps) | Samsung Galaxy SIII (cps) | Huawei Ascend P7 (cps) |
|---|---|---|---|---|
| 226 | 295 | 1070 | 1510 | 1740 |
| 127 | 208 | 597 | 846 | 992 |
| 81.4 | 139 | 380 | 537 | 645 |
| 56.5 | 85.3 | 262 | 370 | 456 |
| 41.5 | 68.3 | 191 | 269 | 342 |
| 31.8 | 54.7 | 144 | 203 | 269 |
| 25.1 | 37.7 | 113 | 158 | 218 |
| 20.4 | 31.9 | 90.4 | 126 | 182 |
| 16.8 | 25.7 | 73.8 | 102 | 156 |
| 14.1 | 29.1 | 60.9 | 84.5 | 135 |

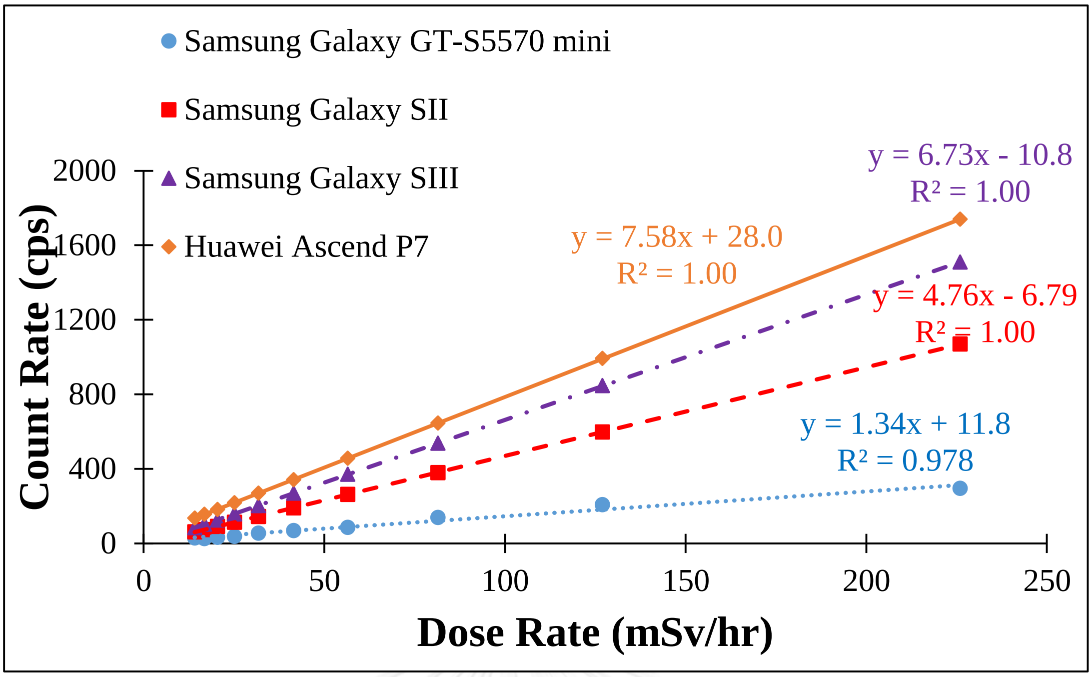


*Figure 49. Comparison of the sensitivity of smartphones by using $^{192}$Ir source*

Based on the Table 9 and Figure 49 above were shown that the count rate increased linearly with increase in the dose rate. However, among these four models of smartphone, Huawei Ascend P7 had the highest sensitivity in measurement of gamma rays. As can be seen in the Table 9 and Figure 49, Huawei Ascend P7 gives the highest count rate at the same gamma-ray dose rate in comparison to others. The second is Samsung Galaxy SIII, third is Samsung Galaxy SII, and the least is Samsung Galaxy GT-S5570. The factors that influent sensitivity of the smartphones are properties of the CMOS sensor inside the cameras, the video recording process and the operation system areas.

## 4.2 Response of Smartphones for $^{137}$Cs

According the result of investigation of the sensitivity of each smartphone by using $^{192}$Ir, we found that among these four models of smartphone, the result from Samsung Galaxy GT-S5570 mini was the lowest one, so the calibration with $^{137}$Cs was done with only three models of smartphone (Samsung Galaxy SII, Samsung Galaxy SIII, and Huawei Ascend P7). The DMSc provided the standard exposure rate, but in this study we focused on equivalent dose rate. Hence, the conversion of exposure rate to equivalent dose rate was shown in appendix D.

*Table 10. Comparison the sensitivity of all smartphones by using $^{137}Cs$*

| Equivalent Dose Rate (mSv/hr) | Samsung Galaxy SII (cps) | Samsung Galaxy SIII (cps) | Huawei Ascend P7 (cps) |
|---|---|---|---|
| 24.2 | 128±1.46 | 135±1.50 | 158±1.62 |
| 6.01 | 29.6±0.701 | 34.9±0.762 | 41.8±0.835 |
| 2.61 | 12.8±0.262 | 14.7±0.495 | 20.3±0.582 |
| 1.44 | 7.31±0.349 | 8.48±0.376 | 12.5±0.456 |
| 0.930 | 4.88±0.285 | 5.54±0.304 | 8.39±0.374 |
| 0.632 | 3.29±0.235 | 4.04±0.259 | 4.51±0.274 |
| 0.465 | 2.36±0.199 | 3.04±0.225 | 3.22±0.232 |

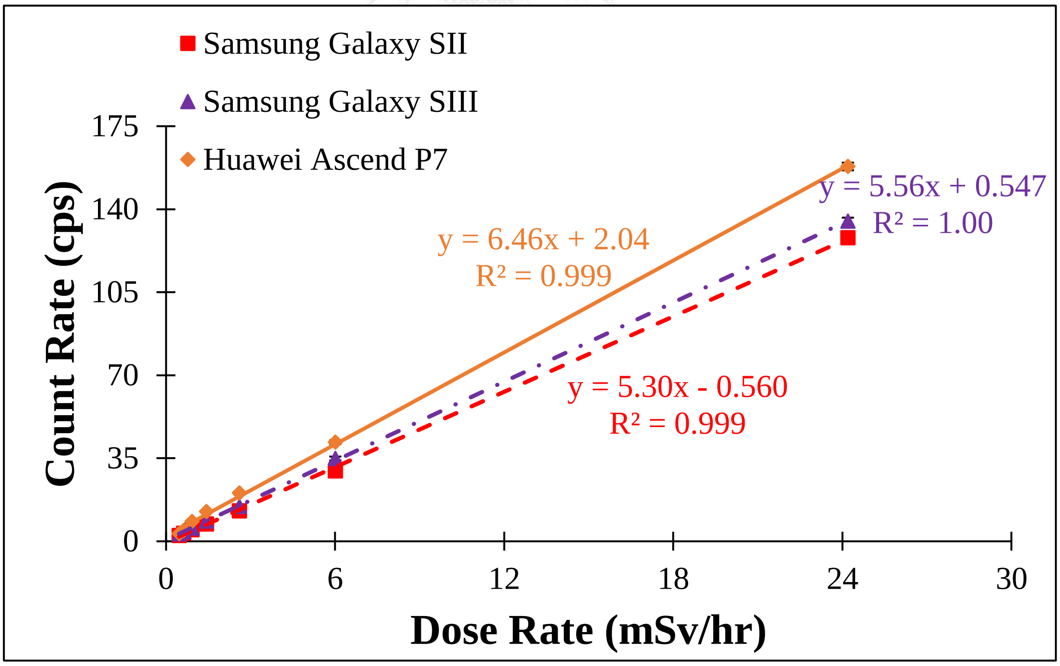


*Figure 50. Comparison sensitivity of all smartphones by using $^{137}Cs$*

Based on the Table 10 and Figure 50 above, Similar to the results of $^{192}Ir$, the count rate was plotted against the dose rate from $^{137}Cs$. It could be also seen that Huawei Ascend P7 still gave the highest result of count rate compare to other smartphones. The second and the third were Samsung Galaxy SIII and Samsung Galaxy SII respectively. Differences in sensitivity are mainly due to similar reasons as mentioned for Ir-192 and Co-60.

## 4.3 Response of Smartphones for $^{60}$Co

Based on the scopes of this study, to investigate the sensitivity of smartphones was also needed to calibrate with gamma source $^{60}$Co. As same as $^{137}$Cs, the three models of smartphone were used in this experiment (Samsung Galaxy SII, Samsung Galaxy SIII, and Huawei Ascend P7). The high exposure rates of Co-60 were provided by the DMSc; however, we converted exposure rate to equivalent dose rate as shown in appendix D.

*Table 11. Comparison the sensitivity of all smartphones by using high equivalent dose rate of $^{60}$Co*

| Equivalent Dose Rate (mSv/hr) | Samsung Galaxy SII (cps) | Samsung Galaxy SIII (cps) | Huawei Ascend P7 (cps) |
|---|---|---|---|
| 8810 | 54800±42.7 | 57900±43.9 | 69500±42.2 |
| 4910 | 31100±32.2 | 32300±32.8 | 38100±35.6 |
| 3130 | 19600±25.6 | 20200±25.9 | 24100±28.3 |
| 2190 | 13500±21.2 | 14100±21.7 | 16600±23.5 |
| 1600 | 9880±18.1 | 10400±18.6 | 12200±20.1 |

We have shown the two results of investigation the sensitivity of smartphones with $^{192}$Ir and $^{137}$Cs which Huawei Ascend P7 could detect gamma rays much more than the other three models. In this calibration with high dose rate of $^{60}$Co, in Table 11 and Figure 51 similar to the results of $^{137}$Cs, the count rate was plotted against the dose rate from $^{60}$Co. It could be also seen that Huawei Ascend P7 still gave the highest result of count rate compare to other smartphones. The second and the third were Samsung

Galaxy SIII and Samsung Galaxy SII respectively. Differences in sensitivity are mainly due to similar reasons as mentioned for $^{192}$Ir and $^{137}$Cs.

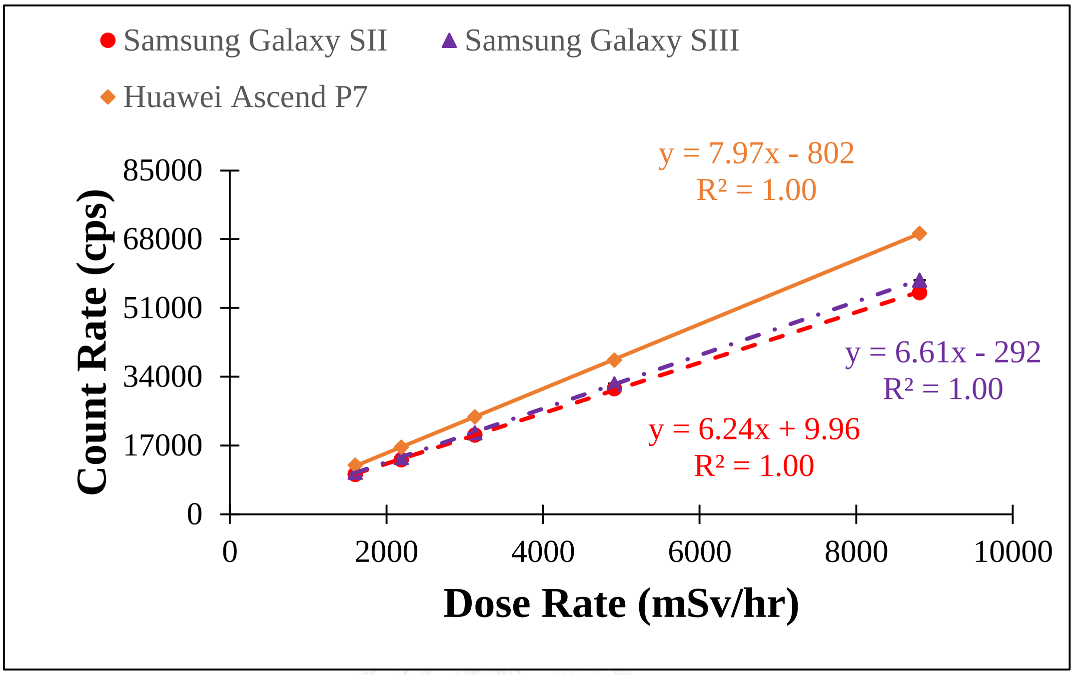


*Figure 51. Comparison the sensitivity of all smartphones by using the high equivalent dose rate of $^{60}$Co*

With the low dose rate of $^{60}$Co, the result in Table 12 and Figure 52 shown Huawei Ascend P7 was still better than Samsung Galaxy SIII to detect gamma rays. All the points of dose rate, the result of count rate from Huawei Ascend P7 were higher than the result from Samsung Galaxy SIII.

*Table 12. Comparison the sensitivity of two smartphones by using low equivalent dose rate of $^{60}$Co*

| Equivalent Dose Rate (mSv/hr) | Samsung Galaxy SIII (cps) | Huawei Ascend P7 (cps) |
|---|---|---|
| 0.288 | 1.86±0.249 | 2.51±0.289 |
| 0.127 | 0.822±0.166 | 0.967±0.180 |
| 0.071 | 0.444±0.122 | 0.511±0.130 |
| 0.046 | 0.267±0.094 | 0.400±0.115 |
| 0.031 | 0.156±0.072 | 0.333±0.105 |

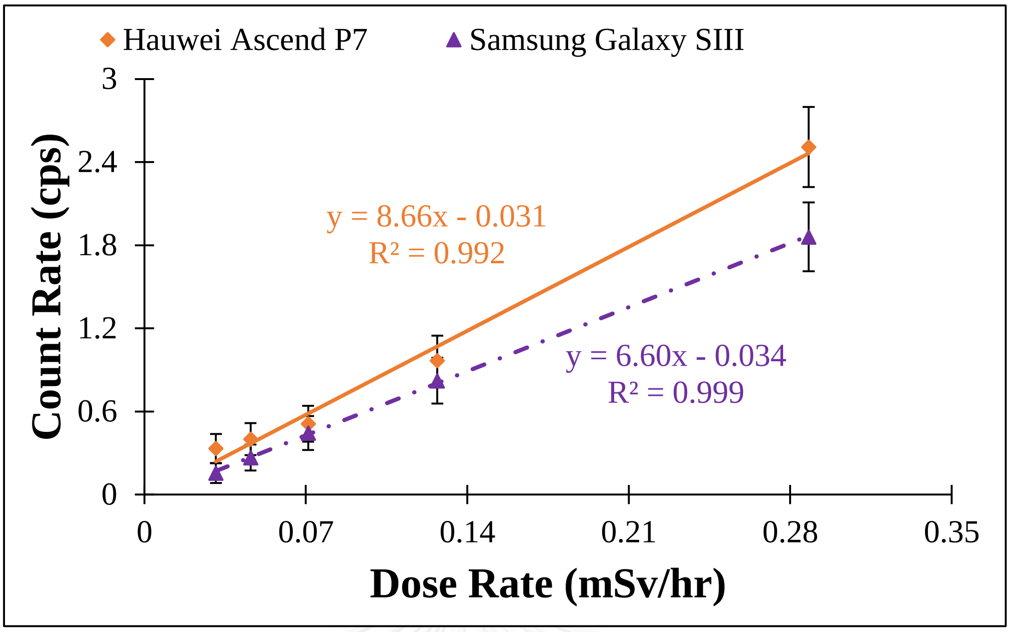


*Figure 52. Comparison the sensitivity of all smartphones by using the low dose rate of $^{60}$Co*

## 4.4 Calibration of Selected Smartphones by Using $^{137}$Cs

According to the investigations of sensitivity of smartphones with $^{192}$Ir, $^{137}$Cs and $^{60}$Co, we could select the best sensitive smartphones (Huawei Ascend P7 and Samsung Galaxy SIII) to calibrate with $^{137}$Cs. The standard exposure rates were given by the SSDL of OAP and they were converted to equivalent dose rate as shown in Appendix D.

Although both Huawei Ascend P7 and Samsung Galaxy SIII were given the perfect results of calibration with $^{137}$Cs, we needed to choose the best sensitive smartphone that could detect gamma rays and give the highest count. So, from the Table 13 and Figure 53 below were shown that Huawei Ascend P7 was the best sensitive smartphone, which could measure gamma rays and gave the result of highest net count.

*Table 13. Comparison of the best calibration for both of these smartphones by using $^{137}Cs$*

| Equivalent Dose Rate (mSv/hr) | Huawei Ascend P7 (cps) | Samsung Galaxy SIII (cps) |
|---|---|---|
| 29.7 | 205±2.62 | 168±2.37 |
| 13.1 | 89.3±1.73 | 73.0±1.56 |
| 7.36 | 51.3±1.31 | 39.7±1.15 |
| 4.69 | 32.2±1.04 | 25.5±0.921 |
| 3.25 | 22.4±0.864 | 18.3±0.781 |

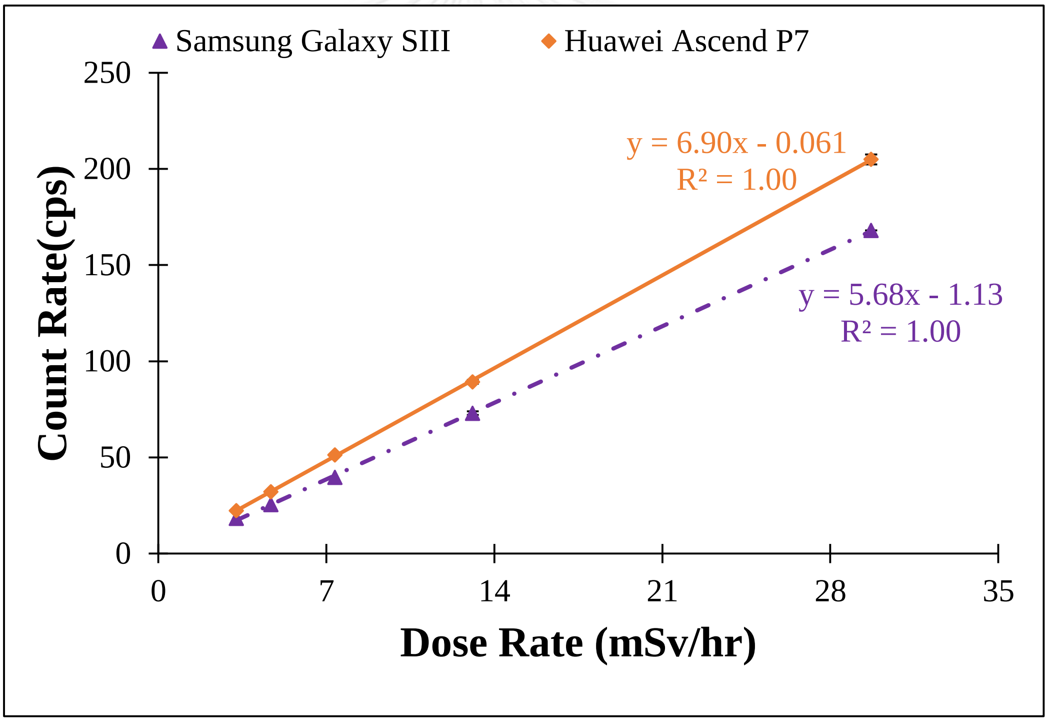


*Figure 53. Comparison the best calibration of both smartphones by using $^{137}Cs$*

## 4.5 Comparison the Equivalent Dose Rate Using Selected Smartphone with the Calibrated Survey Meter and Standard Equivalent Dose rate

From the calibration of smartphones by using $^{137}Cs$, Huawei Ascend P7 was identified as the best sensitive smartphone that could detect gamma rays and gave the highest counts. Hence, the result of Huawei Ascend P7 could be used to find the calibration factor to determine the equivalent dose rate (the detail of calculation was shown in appendix D) for comparison with the standard equivalent dose rate and survey meter. The standard exposure rates and survey meter were given by the SSDL at OAP, and we converted those exposure rates to equivalent dose rate as shown in appendix D.

*Table 14. The equivalent dose rate of $^{137}Cs$ by using Huawei Ascend P7*

| Count rate (cps) | F ((mSv/hr)/cps) | Equivalent Dose Rate (mSv/hr) |
|---|---|---|
| 3.62±0.347 | 0.145 | 0.525 |
| 2.43±0.285 | 0.145 | 0.352 |
| 1.62±0.233 | 0.145 | 0.235 |
| 1.22±0.202 | 0.145 | 0.177 |
| 0.911±0.174 | 0.145 | 0.132 |



After the equivalent dose rate by using smartphone Huawei Ascend P7 was given, next step was to compare this result with the standard equivalent dose rate and the equivalent dose rate from survey meter.

*Table 15. Comparison the standard value of equivalent dose rate with the dose rate from survey meter and smartphone (Huawei Ascend P7) by using $^{137}Cs$*

| Standard Dose Rate (mSv/hr) | Survey meter | | Huawei Ascend P7 | |
|---|---|---|---|---|
| | Dose Rate (mSv/hr) | Discrepancy | Dose Rate (mSv/hr) | Discrepancy |
| 0.545 | 0.547 | +0.002 | 0.525 | -0.020 |
| 0.346 | 0.350 | +0.004 | 0.352 | +0.006 |
| 0.239 | 0.241 | +0.002 | 0.235 | -0.004 |
| 0.176 | 0.176 | 0.000 | 0.177 | +0.001 |
| 0.133 | 0.132 | -0.001 | 0.132 | -0.001 |

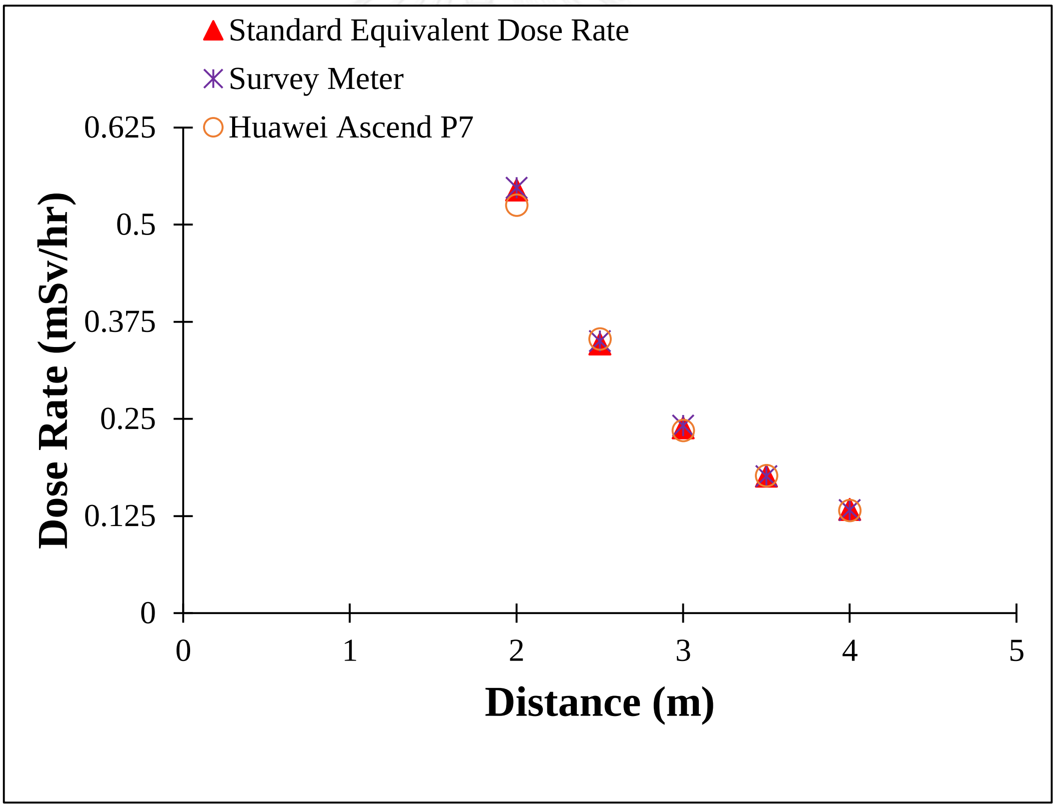


*Figure 54. Comparison the standard equivalent dose rate with the equivalent dose rate from survey meter and smartphone (Huawei Ascend P7) by using $^{137}Cs$*

## 4.6 The Response of Smartphones for Gamma Rays by Using Real-time Counting Software

Although, the result of gamma ray counts by using real-time counting software were less than the result of gamma ray counts from ImageJ, but this software still gave the good result too. From all the results of each calibration, we could use the equation of each result to measure the actual dose rate by using this real-time application software too.

### 4.6.1 Calibration of Samsung Galaxy SIII with $^{137}Cs$

*Table 16. The count rate with dose rate of $^{137}Cs$ by using real-time counting software*

| Equivalent Dose Rate (mSv/hr) | Count Rate (cps) by real-time counting software |
|---|---|
| 24.2 | 5.45±0.301 |
| 6.01 | 1.39±0.152 |
| 2.61 | 0.56±0.096 |
| 1.44 | 0.268±0.067 |
| 0.930 | 0.168±0.053 |
| 0.632 | 0.109±0.043 |
| 0.465 | 0.095±0.039 |

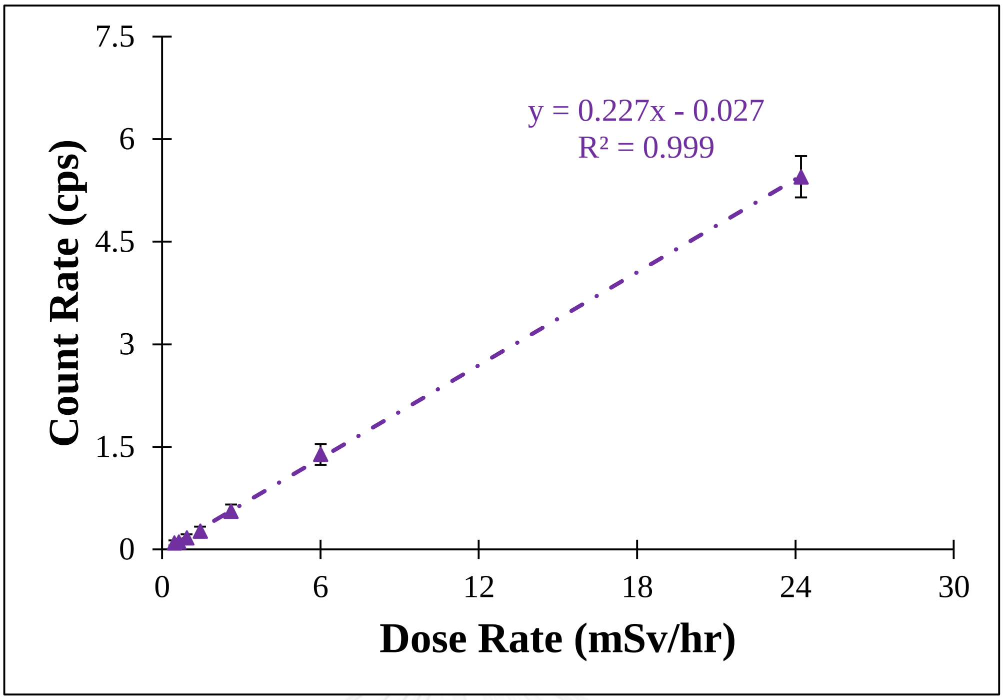


*Figure 55. The count rate (cps) vs the dose rate (mSv/hr) of $^{137}Cs$ by using real-time counting software*

By calibrating with $^{137}Cs$, the result of count by using Samsung Galaxy SIII was increased linearly when the dose rate increased. From the lowest dose rate of 0.465 mSv/hr (count rate 0.095±0.039 cps) to the highest dose rate of 24.2 mSv/hr (count rate 5.45±0.301 cps).

4.6.2 Calibration of Samsung Galaxy SIII with $^{60}Co$

*Table 17. The count rate with the dose rate of $^{60}Co$ by using real-time counting software*

| Equivalent Dose Rate (mSv/hr) | Count Rate (cps) by real-time counting software |
|---|---|
| 8810 | 2380±6.29 |
| 4910 | 1110±4.30 |
| 3130 | 688±3.39 |
| 2190 | 433±2.69 |
| 1600 | 317±2.29 |

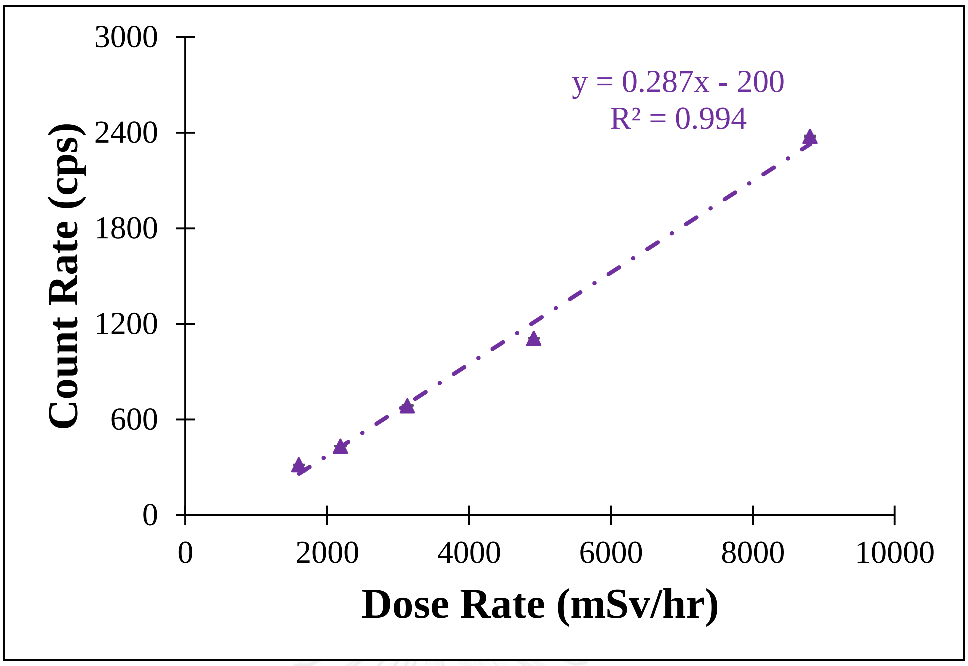


*Figure 56. The count rate (cps) vs the dose rate (mSv/hr) of $^{60}Co$ by using real-time counting software*

With the high dose rate of $^{60}Co$, the result of count by using Samsung Galaxy SIII was quite good too. The result of count rate is increased respectively with the increased of dose rate. From the minimum dose rate of 1600 mSv/hr (count rate 317±2.29 cps) was increased linearly to the maximum dose rate of 8810 mSv/hr (count rate 2380±6.29 cps).



4.6.3 Calibration of Huawei Ascend P7 with $^{192}Ir$

*Table 18. The count rate with the dose rate of $^{192}Ir$ by using real-time counting software*

| Equivalent Dose Rate (mSv/hr) | Count Rate (cps) by real-time counting software |
|---|---|
| 99.9 | 184±4.29 |
| 37.3 | 77.0±2.77 |
| 19.9 | 46.1±2.15 |
| 12.5 | 36.1±1.90 |
| 9.72 | 29.5±1.72 |

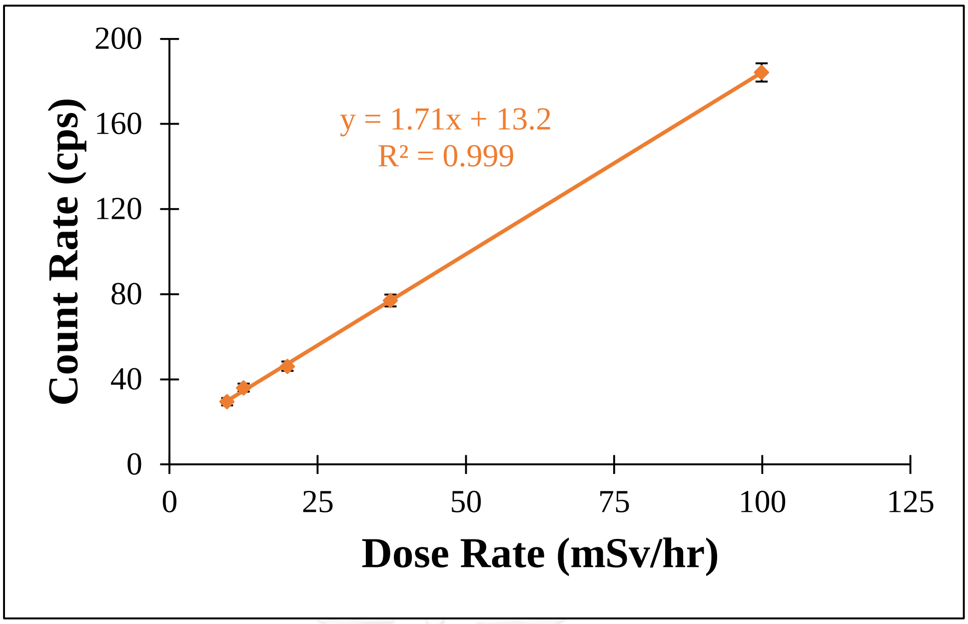


*Figure 57. The count rate (cps) vs the dose rate (mSv/hr) of $^{192}$Ir by using real-time counting software*

With $^{192}$Ir, the calibration by using real-time counting software was done with Huawei Ascend P7. The result of count rate was increased properly with the increased dose rate as linear. From the lowest dose rate of 9.72 mSv/hr (count rate 29.5±1.72 cps) to the highest dose rate of 99.9 mSv/hr (count rate 184±4.29 cps).

# Chapter 5

# CONCLUSION

## 5.1 Conclusion and Discussion

Base on the results from chapter 4, we can conclude that this study was provided the benefits of using smartphones to detect gamma-rays. Firstly, the results of investigation the sensitivity of smartphones (Samsung Galaxy GT-S5570 mini, Samsung Galaxy SII, Samsung Galaxy SIII and Huawei Ascend P7) were shown that the number of gamma ray counts that were measured by these four models of smartphone increased linearly with increasing gamma ray dose rate from $^{192}$Ir. However, Samsung Galaxy GT-S5570 mini was less sensitivity compared to the other three models because the properties (platform, phone processing and camera processing) of this model were very low quality than Samsung Galaxy SII, Samsung Galaxy SIII and Huawei Ascend P7. Therefore, the next investigation the sensitivity of smartphones by using $^{137}$Cs and $^{60}$Co were done with only three models of phone accept Samsung Galaxy GT-S5570.With $^{137}$Cs and high dose rate of $^{60}$Co, the results of gamma ray counts were increased linearly with the increasing standard values of dose rate which were provided by the SSDL at the Department of Medical Sciences. By the way, to confirm that our smartphones were not only sensitive with the high dose rate of gamma rays, we also tested the measurement of low gamma dose rate of $^{60}$Co. The results were clearly shown that the number of gamma ray counts were increased linearly with the increasing low dose rates of $^{60}$Co, which were provided by SSDL at the Office of Atoms for Peace. According to these results, they were totally shown that Huawei Ascend P7 was the most sensitive smartphone with gamma ray, second sensitive smartphone was given to Samsung Galaxy SIII, the third one was Samsung Galaxy SII, and the lowest sensitive smartphone to gamma ray was Samsung Galaxy GT-S5570 mini. Totally, the smartphones properties (platform, phone processing, and camera processing) affected to the result of gamma ray measurement.

The calibration of selected smartphones with $^{137}Cs$ were done with the two models of phone, Huawei Ascend P7 and Samsung Galaxy SIII. The purpose to do this calibration was to choose the best calibration of smartphone with the highest result of number of gamma ray counts. So, the result from chapter 4 shown that both of smartphones were perfectly given the best linearity of count rates with the increased dose rates, but Huawei Ascend P7 could give the result of gamma ray counts more than Samsung Galaxy SIII. Then Huawei Ascend P7 was chosen to be the standard calibrated smartphone with gamma ray measurement. It was tested in measurement of gamma-ray dose rate in comparison with the standard values and with the dose rate survey meter. The results were very satisfactory. Application software for Android smartphones was finally developed so that the number of bright spots could be simultaneously counted and converted to gamma-ray dose rate to display on the smartphones.

It is clearly shown that with our methods, smartphones are better than some hand-held survey meters in linearity wider dose rate range because our smartphones could detect gamma ray dose rate from the low to the very high range and gave the very good results. However, some types of survey meters could not measure the very high dose rate. They can be damaged or given the wrong result of gamma ray dose rate, but our smartphones indicate the good results and we still can use those smartphones as normal. Hence, we assume that smartphone is very useful in daily life, it is not as same as survey meter that can use only radiation measurement, but people can enjoy with their smartphone and the price is also reasonable.

## 5.2 Recommendation

Because of the limitation of time and budget, we could not select many models of smartphone to study, so we hope that the future study will test more with many models of smartphone and compare with those we have been used in this study. Moreover, application software for Android smartphones was finally developed, so for radiation workers can easily use their smartphones perform with this real-time application software instead of the heavy survey meter to measure the gamma ray dose rate while they are working in radiation field. The appropriated calibration is required for different models of smartphone; however, even the same model of smartphone may have different sensitivity, and each of them needs appropriate calibration as normally do with dosimeters and survey meters. These techniques will help them to avoid the high risk from radiation exposure, both in normal working condition and in case of emergency.

## REFERENCES


[1] Joshua J., C., D. Kurt W., and W. Jayson, Using CMOS Sensors in a Cellphone for Gamma Detection and Classification. Using CMOS Sensors in a Cellphone for Gamma Detection and Classification, 2014: p. 26.

[2] ANSTO Smartphone Radiation Detector App Tests Positive. 2014. 4.

[3] Gumiela, M. and R. Kozik, Studies of the applicability of CMOS and CCD sensors for detection, dosimetry and imaging of alpha, beta, gamma, x-ray and proton beam spots. Studies of the applicability of CMOS and CCD sensors for detection, dosimetry and imaging of alpha, beta, gamma, x-ray and proton beam spots, 2012.

[4] Iemsumang, K., Development of an Iridium-192 Gamma Radiography System Using PI-200 Fluorescent Screen Coupled with Digital Camera, in Nuclear Engineering. 2012, Chulalongkorn: Chulalongkorn University. p. 71.

[5] Drukier, G.A., et al., Low Cost, Pervasive Detection of Radiation Threats, in IEEE International Conference. 2011, IEEE. p. 7.

[6] Abdalla, M.A., PIXEL DETECTORS AND ELECTRONICS FOR HIGH ENERGY RADIATION IMAGING, in Electronics. 2001, The Royal Institute of Technology. p. 69.

[7] Reilly, D., The Origin of Gamma Rays, in Passive Nondestructive Assay of Nuclear Materials, D. Reilly, N. Ensslin, and J. Hastings Smith, Editors. 1991, U.S. Government Printing Office: Washington, DC 20013-7082, United States. p. 24.

[8] Nelson, G. and D. Reilly, Gamma-Ray Interactions with Matter, in Passive Nondestructive Assay of Nuclear Materials, D. Reilly, N. Ensslin, and J. Hastings Smith, Editors. 1991, U.S. Government Printing Office: Washington, DC 20013-7082, United States. p. 11.

[9] Cember, H. and T.E. Jonhson, Introduction to Health Physics. 2009, The McGraw-Hill Companies, Inc.

[10] Lamarsh, J.R. and A.J. Baratta, Introduction to Nuclear Engineering, M.J. Horton, L. Curless, and E. Katchmar, Editors. 2001, Prentice-Hall, Inc.: Upper Saddle River, New Jersey 07458.

[11] (IAEA), I.A.E.A., GAMMA IRRADIATORS FOR RADIATION PROCESSING. International Atomic Energy Agency: Vienna, Austria. p. 46.

[12] (IAEA), I.A.E.A., TRENDS IN RADIATION STERILIZATION OF HEALTH CARE PRODUCTS. 2008, International Atomic Energy Agency: Wagramer Strasse 5, P.O. Box 100, 1400 Vienna, Austria. p. 278.

[13] Association, I.I., Benificial Uses of Cobalt-60. 2006.

[14] (CDC), C.f.D.C.a.P., Radiation Emergencies, H.a.H. Services, Editor. 2004. p. 2.

[15] ISOFLEX. Isotopes for Science, Medicine and Industry. 2015 30 August 2015.

[16] Hayward, P. and D. Currie, RADIOGRAPHY OF WELDS USING SELENIUM 75, IR 192 AND X-RAYS, in Asia-Pacific Conference on NDT. 2006: Auckland, New Zealand. p. 5.

[17] Shilton, D.M.G., CChem, and MRSC Advance, Second Generation Selenium-75 Gamma Radiography Sources.

[18] Loft, S.M., I.P. Coles, and R.G. Dale, The potential of ytterbium 169 in brachytherapy: a brief physical and radiobiological assessment. The British Journal of Radiology, 1992: p. 5.

[19] (CDC), C.f.D.C.a.P., Radioisotope Brief: Iodine-131 (I-131), U.S.D.o.H.a.H. Services, Editor., CDC: 1600 Clifton Road Atlanta, GA 30329-4027 USA.

[20] EPA Radiation: Facts, Risks and Realities. Radiation: Facts, Risks and Realities, 2012. 17.

[21] Zamanian, A. and C. Hardiman, Electromagnetic Radiation and Human Health: A Review of Sources and Effects, in High Frequency Electronics. 2005.

[22] ACS X-rays, Gamma Rays, and Cancer Risk. 2014. 15.

[23] Niu, S. Radiation Protection of Workers. SafeWork Information Note 2011.

[24] ‘ICRP and . Radiological protection in paediatric diagnostic and interventional radiology. 2013.

[25] Sher, R. and S. Untermyer, The Detection of Fissionable Materials by Nondestructive Means. 1980, 555 North Kensington Avenue, La Grange Park, Illinois, USA: The American Nuclear Society.

[26] Hastings A. Smith, J. and M. Lucas, Gamma-Ray Detectors, in Passive Nondestructive Assay of Nuclear Materials, D. Reilly, N. Ensslin, and J. Hastings Smith, Editors. 1991, U.S. Government Printing Office: Washington, DC 20013-7082, United States. p. 19.

[27] Bigas, M., et al., Review of CMOS image sensors. Review of CMOS image sensors, 2006: p. 19.

[28] SONY CCD and CMOS Image Sensors: A Comprehensive Guide for Professional Videographers.

[29] Makowski, D., The Impact of Radiation on Electronic Devices with the Special Consideration of Neutron and Gamma Radiation Monitoring, in Microelectronics and Computer Science. 2006, Technical University of Łódź.

[30] Goiffon, V., et al., Radiation Damages in CMOS Image Sensors: Testing and Hardening Challenges Brought by Deep Sub-Micrometer CIS Processes. Radiation Damages in CMOS Image Sensors: Testing and Hardening Challenges Brought by Deep Sub-Micrometer CIS Processes, 2010: p. 13.

[31] IAEA, Handbook on Calibration of Radiation Protection Monitoring Instruments. TECHNICAL REPORTS. 1971, International Atomic Energy Agency, Karntner Ring 11, P.O. Box 590, A-1011 Vienna, Austria: IAEA. 95.

[32] Ferreira, T. and W. Rasband, ImageJ/ FIJI 1.46. 2012. p. 198.

# APPENDICES

## Appendix A: Hand-held Gamma and Neutron Search Instrument HDS-101 GN

The hand-held radiation detector HDS-101 GN is an ultra-sensitive gamma/neutron radiation alarming detector. It is designed to detect, locate, quantify and identify any radioactive materials (special nuclear materials) and to response to incidents involving Radiological Dispersal Devices. It can be used as a low cost permanent detector in a room or for a walk through passage when placed into the SPIR detect system. This product is ideally suited for first responders, border control, customs inspection and security of critical infrastructure applications.

### Technical Specifications

| Gamma Detector | |
|---|---|
| Type | CsI(Tl) crystal |
| Energy range | 30 keV to 3 MeV |
| Sensitivity | Typical 1400 cps per μSv/hr for Cs-137 source |
| Spectrum | 512 channels |
| Maximum displayed count rate | 99999 cps |
| Measurement range | 10 nSv/hr to 100 μSv/hr (Cs-137)<br>10 nSv/hr to 30 μSv/hr (Am-241) |

| Gamma Detector_ High range | |
|---|---|
| Type | Silicon Diode |
| Energy range | 50 keV to 6 MeV |
| Sensitivity | Typical 0.03 cps per μSv/hr for Cs-137 source |
| Measurement range | 10 μSv/hr to 10 mSv/hr nominal<br>10 μSv/hr to 100 mSv/hr during 5 min max |
| Measurement range with CsI detector damage risk | Up to 8 Sv/hr |

**Appendix B: The certificate of ionization chamber with display unit from the Office of Atoms for Peace**

**Physikalisch-Technische Bundesanstalt** PTB

Braunschweig und Berlin

Kalibrierschein

*Calibration Certificate*

| | | |
|---|---|---|
| Gegenstand: *Object:* | Ionisation chamber with display unit | |
| Hersteller: *Manufacturer:* | Standard Imaging Inc.<br>Middelton | |
| Typ: *Type:* | A6 REF 92716<br>MAX 4000 REF90015 | S/N XQ063052<br>S/N E062682 |
| Kennnummer: *Serial No.:* | see above | |
| Auftraggeber: *Applicant:* | Bureau of Technical Support of Safety Regulation<br>Office of Atoms for Peace (OAP)<br>16 Vibhavadi Rangsit Rd., Chatuchak<br>Bangkok 10900, Thailand | |
| Anzahl der Seiten: *Number of pages:* | 5 | |
| Geschäftszeichen: *Reference No.:* | 6.25 - 48/12K | |
| Kalibrierzeichen: *Calibration mark:* | chamber 60218-12, display unit 60216-12 | |
| Datum der Kalibrierung: *Date of calibration:* | 2012-08-13 to 2012-08-28 | |

Im Auftrag *On behalf of PTB* — Braunschweig, 2012-08-29 — Im Auftrag *On behalf of PTB*

Siegel *Seal*

Dr. L. Büermann — Warkehr

Kalibrierscheine ohne Unterschrift und Siegel haben keine Gültigkeit. Dieser Kalibrierschein darf nur unverändert weiterverbreitet werden. Auszüge bedürfen der Genehmigung der Physikalisch-Technischen Bundesanstalt.
*Calibration Certificates without signature and seal are not valid. This Calibration Certificate may not be reproduced other than in full. Extracts may be taken only with the permission of the Physikalisch-Technische Bundesanstalt.*

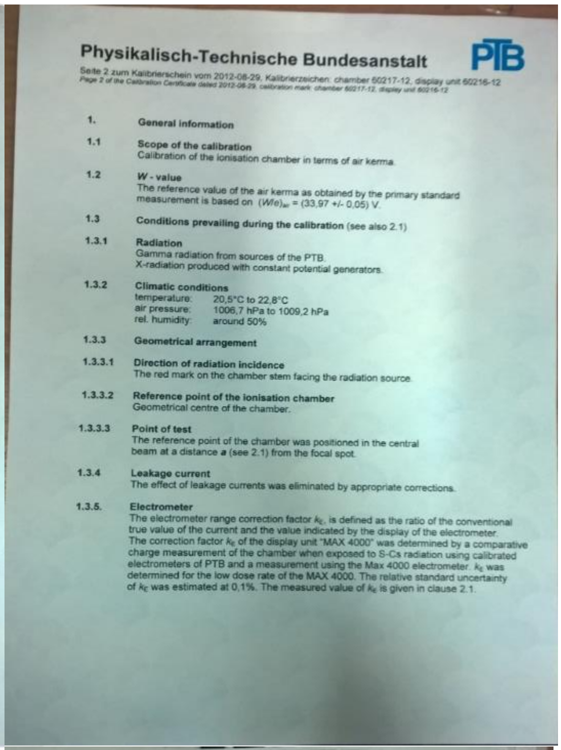

**Physikalisch-Technische Bundesanstalt** PTB

Seite 2 zum Kalibrierschein vom 2012-08-29, Kalibrierzeichen: chamber 60217-12, display unit 60216-12
*Page 2 of the Calibration Certificate dated 2012-08-29, calibration mark: chamber 60217-12, display unit 60216-12*

**1. General information**

**1.1 Scope of the calibration**
Calibration of the ionisation chamber in terms of air kerma.

**1.2 *W* - value**
The reference value of the air kerma as obtained by the primary standard measurement is based on $(W/e)_{air}$ = (33,97 +/- 0,05) V.

**1.3 Conditions prevailing during the calibration** (see also 2.1)

**1.3.1 Radiation**
Gamma radiation from sources of the PTB.
X-radiation produced with constant potential generators.

**1.3.2 Climatic conditions**
temperature: 20,5°C to 22,8°C
air pressure: 1006,7 hPa to 1009,2 hPa
rel. humidity: around 50%

**1.3.3 Geometrical arrangement**

**1.3.3.1 Direction of radiation incidence**
The red mark on the chamber stem facing the radiation source.

**1.3.3.2 Reference point of the ionisation chamber**
Geometrical centre of the chamber.

**1.3.3.3 Point of test**
The reference point of the chamber was positioned in the central beam at a distance ***a*** (see 2.1) from the focal spot.

**1.3.4 Leakage current**
The effect of leakage currents was eliminated by appropriate corrections.

**1.3.5. Electrometer**
The electrometer range correction factor $k_E$, is defined as the ratio of the conventional true value of the current and the value indicated by the display of the electrometer. The correction factor $k_E$ of the display unit "MAX 4000" was determined by a comparative charge measurement of the chamber when exposed to S-Cs radiation using calibrated electrometers of PTB and a measurement using the Max 4000 electrometer. $k_E$ was determined for the low dose rate of the MAX 4000. The relative standard uncertainty of $k_E$ was estimated at 0,1%. The measured value of $k_E$ is given in clause 2.1.

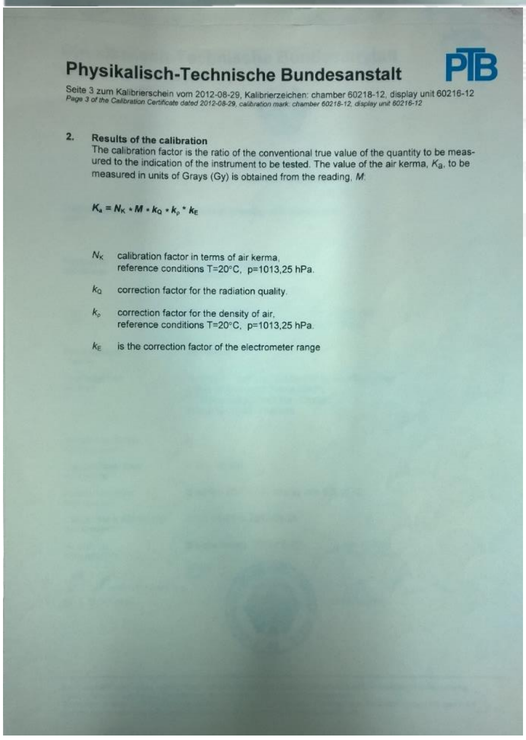

**Physikalisch-Technische Bundesanstalt** PTB

Seite 3 zum Kalibrierschein vom 2012-08-29, Kalibrierzeichen: chamber 60218-12, display unit 60216-12
*Page 3 of the Calibration Certificate dated 2012-08-29, calibration mark: chamber 60218-12, display unit 60216-12*

**2. Results of the calibration**
The calibration factor is the ratio of the conventional true value of the quantity to be measured to the indication of the instrument to be tested. The value of the air kerma, $K_a$, to be measured in units of Grays (Gy) is obtained from the reading, *M*:

$$K_a = N_K * M * k_Q * k_\rho * k_E$$

$N_K$ calibration factor in terms of air kerma, reference conditions T=20°C, p=1013,25 hPa.

$k_Q$ correction factor for the radiation quality.

$k_\rho$ correction factor for the density of air, reference conditions T=20°C, p=1013,25 hPa.

$k_E$ is the correction factor of the electrometer range

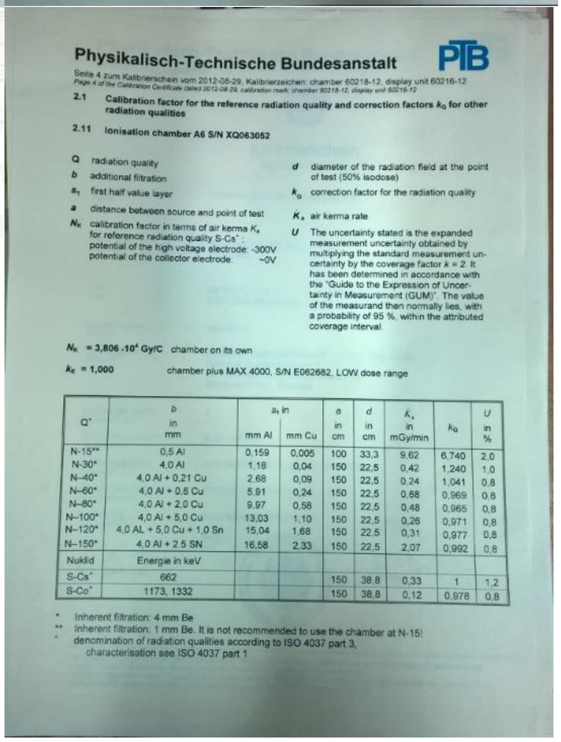

**Physikalisch-Technische Bundesanstalt** PTB

Seite 4 zum Kalibrierschein vom 2012-08-29, Kalibrierzeichen: chamber 60218-12, display unit 60216-12
*Page 4 of the Calibration Certificate dated 2012-08-29, calibration mark: chamber 60218-12, display unit 60216-12*

**2.1 Calibration factor for the reference radiation quality and correction factors $k_Q$ for other radiation qualities**

**2.11 Ionisation chamber A6 S/N XQ063052**

- **Q** radiation quality
- ***b*** additional filtration
- $s_1$ first half value layer
- ***a*** distance between source and point of test
- $N_K$ calibration factor in terms of air kerma $K_a$ for reference radiation quality S-Cs*; potential of the high voltage electrode: -300V; potential of the collector electrode: ~0V
- ***d*** diameter of the radiation field at the point of test (50% isodose)
- $k_Q$ correction factor for the radiation quality
- $\dot{K}_a$ air kerma rate
- ***U*** The uncertainty stated is the expanded measurement uncertainty obtained by multiplying the standard measurement uncertainty by the coverage factor $k$ = 2. It has been determined in accordance with the "Guide to the Expression of Uncertainty in Measurement (GUM)". The value of the measurand then normally lies, with a probability of 95 %, within the attributed coverage interval.

$N_K$ **= 3,806 ·10⁴ Gy/C** chamber on its own

$k_E$ **= 1,000** chamber plus MAX 4000, S/N E062682, LOW dose range

| Q* | *b* in mm | $s_1$ in mm Al | $s_1$ in mm Cu | *a* in cm | *d* in cm | $\dot{K}_a$ in mGy/min | $k_Q$ | *U* in % |
|---|---|---|---|---|---|---|---|---|
| N-15** | 0,5 Al | 0,159 | 0,005 | 100 | 33,3 | 9,62 | 6,740 | 2,0 |
| N-30* | 4,0 Al | 1,18 | 0,04 | 150 | 22,5 | 0,42 | 1,240 | 1,0 |
| N–40* | 4,0 Al + 0,21 Cu | 2,68 | 0,09 | 150 | 22,5 | 0,24 | 1,041 | 0,8 |
| N–60* | 4,0 Al + 0,6 Cu | 5,91 | 0,24 | 150 | 22,5 | 0,68 | 0,969 | 0,8 |
| N–80* | 4,0 Al + 2,0 Cu | 9,97 | 0,58 | 150 | 22,5 | 0,48 | 0,965 | 0,8 |
| N–100* | 4,0 Al + 5,0 Cu | 13,03 | 1,10 | 150 | 22,5 | 0,26 | 0,971 | 0,8 |
| N–120* | 4,0 AL + 5,0 Cu + 1,0 Sn | 15,04 | 1,68 | 150 | 22,5 | 0,31 | 0,977 | 0,8 |
| N–150* | 4,0 Al + 2,5 SN | 16,58 | 2,33 | 150 | 22,5 | 2,07 | 0,992 | 0,8 |
| Nuklid | Energie in keV | | | | | | | |
| S-Cs* | 662 | | | 150 | 38,8 | 0,33 | 1 | 1,2 |
| S-Co* | 1173, 1332 | | | 150 | 38,8 | 0,12 | 0,978 | 0,8 |

* Inherent filtration: 4 mm Be
** Inherent filtration: 1 mm Be. It is not recommended to use the chamber at N-15!
* denomination of radiation qualities according to ISO 4037 part 3, characterisation see ISO 4037 part 1

## Appendix C: Setting zero background of Threshold

Based on the procedure in Chapter 3 of ImageJ, below is the method to set the threshold by using standard images before radiation exposure.

1. Inversing step: each images were inversed

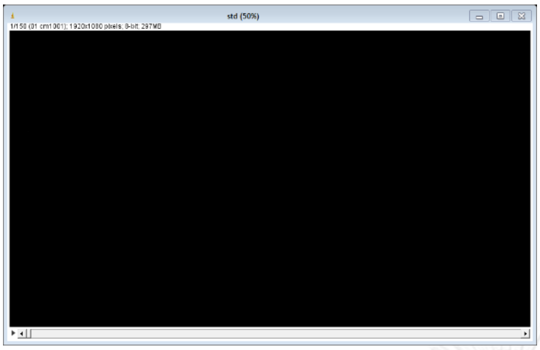

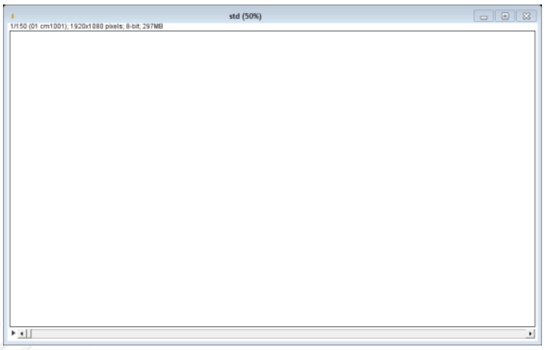

2. Setting Threshold: in this step, each background threshold setting were set many times to get the result as zero count.

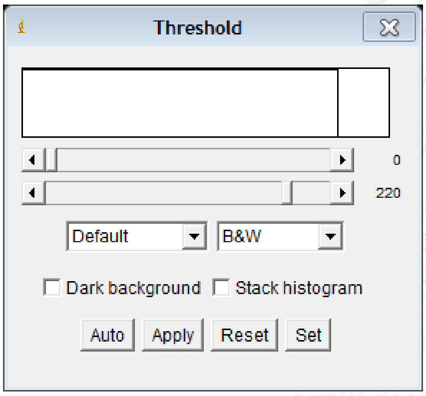


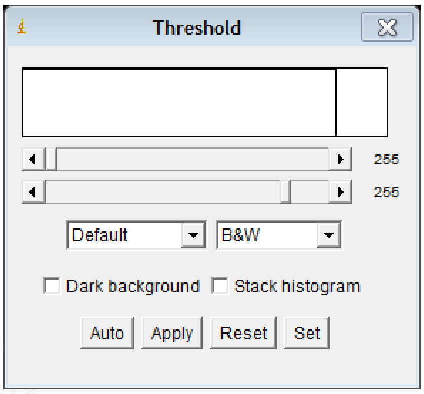


3. after particles analyzing, we got the result as zero count, so mean that the threshold for this zero count were applied for the images sample procedure.

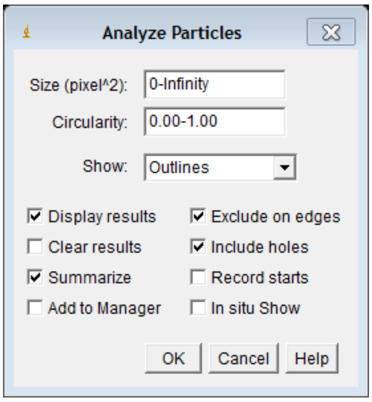

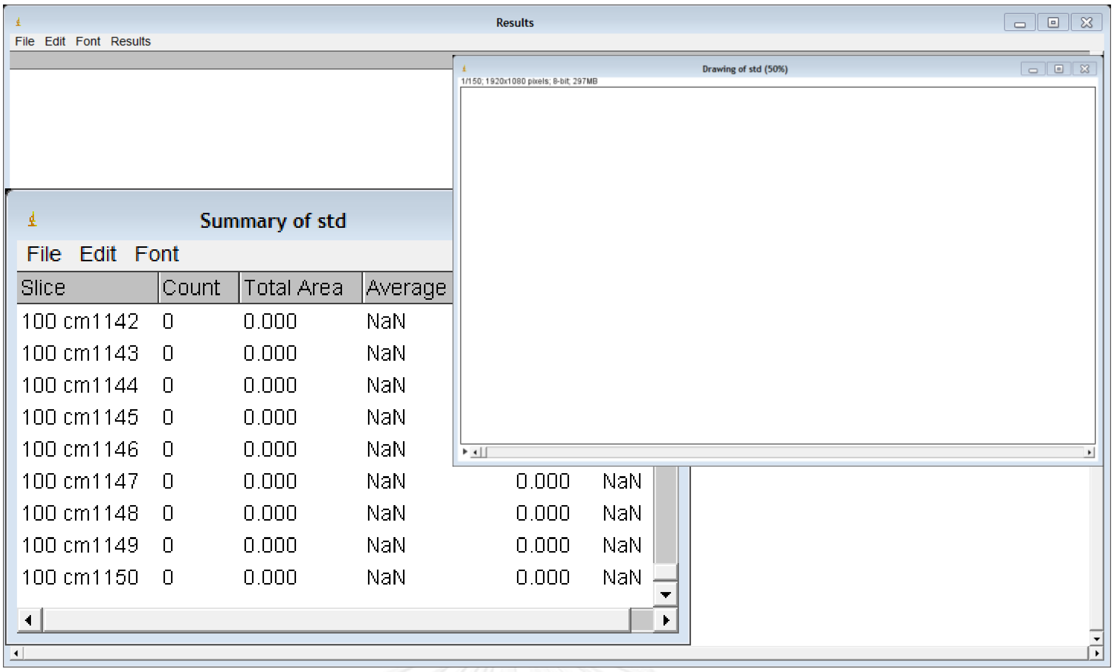
Results
File Edit Font Results
Drawing of std (50%)
Summary of std
File Edit Font
Slice Count Total Area Average
100 cm1142 0 0.000 NaN
100 cm1143 0 0.000 NaN
100 cm1144 0 0.000 NaN
100 cm1145 0 0.000 NaN
100 cm1146 0 0.000 NaN
100 cm1147 0 0.000 NaN 0.000 NaN
100 cm1148 0 0.000 NaN 0.000 NaN
100 cm1149 0 0.000 NaN 0.000 NaN
100 cm1150 0 0.000 NaN 0.000 NaN

## Appendix D: Results

1. The investigation sensitivity of smartphones by using Ir-192

### 1.1. Exposure Rate Calculation

Exposure rate = $\Gamma \times \frac{A}{d^2}$ which,

Exposure rate (R/hr)

$\Gamma$: specific gamma ray constant (R.m$^2$/ Ci.hr)

A: current activity (Ci)

d: distance (m)

We have $\Gamma$ of Ir-192 = 0.44 R/Ci.hr at 1 m, $t_{1/2}$ = 74.3 days

$A = A_0 e^{-\lambda t}$, which $\lambda = \ln 2/t_{1/2}$

$A_0$ = 12.44 Ci on 21$^{st}$ October 2014

So, on 23$^{rd}$ January 2015, t = 92 days, A = 5.27 Ci

On 19$^{th}$ February 2015, t = 118 days, so A = 4.14 Ci

And on 10$^{th}$ March 2015, t = 139 days, A = 3.40 Ci

The result of exposure rate was shown in the table below:

| Distance (m) | Exposure Rate (R/hr), 23$^{rd}$ January 2015 | Exposure Rate (R/hr), 19$^{th}$ February 2015 | Exposure rate (R/hr), 10$^{th}$ March 2015 |
|---|---|---|---|
| 0.300 | 25.8 | 20.2 | 16.6 |
| 0.400 | 14.5 | 11.4 | 9.36 |
| 0.500 | 9.28 | 7.28 | 5.99 |
| 0.600 | 6.44 | 5.06 | 4.16 |
| 0.700 | 4.73 | 3.72 | 3.06 |
| 0.800 | 3.62 | 2.85 | 2.34 |
| 0.900 | 2.86 | 2.25 | 1.85 |
| 1.00 | 2.32 | 1.82 | 1.5 |
| 1.10 | 1.92 | 1.5 | 1.24 |
| 1.20 | 1.61 | 1.26 | 1.04 |

## 1.2.Converting exposure rate to equivalent dose rate

By using the conversion from 2.1.6 1 Sv/hr = 1 Gy/hr = 114 R/hr, we can convert the exposure rate to equivalent dose rate as:

| Exposure Rate (R/hr) | Equivalent Dose Rate (mSv/hr) |
|---|---|
| 25.8 | 226 |
| 14.5 | 127 |
| 9.28 | 81.4 |
| 6.44 | 56.5 |
| 4.73 | 41.5 |
| 3.62 | 31.8 |
| 2.86 | 25.1 |
| 2.32 | 20.4 |
| 1.92 | 16.8 |
| 1.61 | 14.1 |

| Exposure Rate(R/hr) | Equivalent Dose Rate (mSv/hr) |
|---|---|
| 20.2 | 177 |
| 11.4 | 100 |
| 7.28 | 63.9 |
| 5.06 | 44.4 |
| 3.72 | 32.6 |
| 2.85 | 25.0 |
| 2.25 | 19.7 |
| 1.82 | 15.9 |
| 1.50 | 13.2 |
| 1.26 | 11.1 |

| Exposure Rate (R/hr) | Equivalent Dose Rate (mSv/hr) |
|---|---|
| 16.6 | 146 |
| 9.36 | 82.1 |
| 5.99 | 52.5 |
| 4.16 | 36.5 |
| 3.06 | 26.8 |
| 2.34 | 20.5 |
| 1.85 | 16.2 |
| 1.49 | 13.1 |
| 1.24 | 10.9 |
| 1.04 | 9.12 |

## 1.3.Total counts of gamma rays Samsung Galaxy GT-S5570 mini

The number of counts were counted in 30 seconds and iterated for three times.

| Equivalent Dose Rate (mSv/hr) | 1st | 2nd | 3rd | Average |
|---|---|---|---|---|
| 226 | 8861 | 8826 | 8834 | 8840 |
| 127 | 6203 | 6264 | 6282 | 6250 |
| 81.4 | 4141 | 4160 | 4210 | 4170 |
| 56.5 | 2581 | 2511 | 2589 | 2560 |
| 41.5 | 2009 | 2069 | 2071 | 2050 |
| 31.8 | 1620 | 1661 | 1639 | 1640 |
| 25.1 | 1121 | 1173 | 1097 | 1130 |
| 20.4 | 1001 | 931 | 940 | 957 |
| 16.8 | 770 | 750 | 796 | 772 |
| 14.1 | 880 | 864 | 876 | 873 |

1.4.Total counts of gamma rays by using Samsung Galaxy SII

The number of counts were counted in 30 seconds and iterated for three times.

| Equivalent Dose Rate (mSv/hr) | 1st | 2nd | 3rd | Average |
|---|---|---|---|---|
| 177 | 25651 | 25580 | 25570 | 25600 |
| 100 | 13621 | 13584 | 13596 | 13600 |
| 63.9 | 8081 | 8050 | 8048 | 8060 |
| 44.4 | 5943 | 5961 | 5915 | 5940 |
| 32.6 | 4306 | 4302 | 4323 | 4310 |
| 25 | 3471 | 3425 | 3483 | 3460 |
| 19.7 | 2800 | 2833 | 2918 | 2850 |
| 15.9 | 2373 | 2364 | 2374 | 2370 |
| 13.2 | 1999 | 1951 | 2021 | 1990 |
| 11.1 | 1633 | 1630 | 1718 | 1660 |

1.5. Total counts of gamma rays by using Huawei Ascend P7

The number of counts were counted in 30 seconds and iterated for three times.

| Equivalent Dose Rate(mSv/hr) | 1st | 2nd | 3rd | Average |
|---|---|---|---|---|
| 177 | 41250 | 41181 | 41170 | 41200 |
| 100 | 23354 | 23281 | 23264 | 23300 |
| 63.9 | 15511 | 15479 | 15509 | 15500 |
| 44.4 | 11180 | 11231 | 11190 | 11200 |
| 32.6 | 8345 | 8301 | 8345 | 8330 |
| 25 | 6371 | 6399 | 6369 | 6380 |
| 19.7 | 5246 | 5231 | 5244 | 5240 |
| 15.9 | 4585 | 4562 | 4562 | 4570 |
| 13.2 | 3721 | 3701 | 3709 | 3710 |
| 11.1 | 3282 | 3310 | 3277 | 3290 |

1.6.Total counts of gamma rays by using Samsung Galaxy SIII

The number of counts were counted in 30 seconds and iterated for three times.

| Equivalent Dose Rate(mSv/hr) | 1st | 2nd | 3rd | Average |
|---|---|---|---|---|
| 146 | 30296 | 30315 | 30289 | 30300 |
| 82.1 | 14509 | 14520 | 14472 | 14500 |
| 52.5 | 9342 | 9381 | 9356 | 9360 |
| 36.5 | 6743 | 6770 | 6706 | 6740 |
| 26.8 | 5193 | 5160 | 5186 | 5180 |
| 20.5 | 3902 | 3891 | 3938 | 3910 |
| 16.2 | 3083 | 3103 | 3085 | 3090 |
| 13.1 | 2749 | 2801 | 2789 | 2780 |
| 10.9 | 2353 | 2386 | 2342 | 2360 |
| 9.12 | 2035 | 2012 | 2044 | 2030 |

1.7.Total counts of gamma rays by using Huawei Ascend P7

The number of counts were counted in 30 seconds and iterated for three times.

| Equivalent Dose Rate(mSv/hr) | 1st | 2nd | 3rd | Average |
|---|---|---|---|---|
| 146 | 34041 | 33985 | 33973 | 34000 |
| 82.1 | 18233 | 18199 | 18169 | 18200 |
| 52.5 | 11790 | 11798 | 11811 | 11800 |
| 36.5 | 8622 | 8594 | 8615 | 8610 |
| 26.8 | 6659 | 6692 | 6688 | 6680 |
| 20.5 | 5170 | 5155 | 5246 | 5190 |
| 16.2 | 3976 | 4001 | 3992 | 3990 |
| 13.1 | 3672 | 3688 | 3651 | 3670 |
| 10.9 | 3012 | 2990 | 2997 | 3000 |
| 9.12 | 2580 | 2591 | 2688 | 2620 |

## 2. The investigation sensitivity of smartphones by using Cs-137

### 2.1. Converting Exposure rate to equivalent dose rate

By using the conversion from 2.1.6 1 Sv/hr = 1 Gy/hr = 114 R/hr, we can convert the exposure rate to equivalent dose rate as:

| Exposure Rate (R/hr) | Equivalent Dose Rate (mSv/hr) |
|---|---|
| 2.76 | 24.2 |
| 0.685 | 6.01 |
| 0.298 | 2.61 |
| 0.164 | 1.44 |
| 0.106 | 0.930 |
| 0.072 | 0.632 |
| 0.053 | 0.465 |

### 2.2. Total counts of gamma rays by using Samsung Galaxy SII

The number of counts were counted in 60 seconds and iterated for three times.

| Equivalent Dose Rate (mSv/hr) | 1st | 2nd | 3rd | Average |
|---|---|---|---|---|
| 24.2 | 7853 | 7838 | 7363 | 7680 |
| 6.01 | 1810 | 1772 | 1740 | 1770 |
| 2.61 | 787 | 781 | 739 | 769 |
| 1.44 | 403 | 465 | 447 | 438 |
| 0.93 | 292 | 302 | 284 | 293 |
| 0.632 | 193 | 196 | 204 | 198 |
| 0.465 | 140 | 136 | 149 | 142 |

## 2.3. Total counts of gamma rays by using Samsung Galaxy SIII

The number of counts were counted in 60 seconds and iterated for three times.

| Equivalent Dose Rate (mSv/hr) | 1st | 2nd | 3rd | Average |
|---|---|---|---|---|
| 24.2 | 8204 | 8031 | 8075 | 8100 |
| 6.01 | 2067 | 2043 | 2172 | 2094 |
| 2.61 | 862 | 906 | 879 | 882 |
| 1.44 | 533 | 498 | 496 | 509 |
| 0.93 | 357 | 312 | 328 | 332 |
| 0.632 | 245 | 248 | 234 | 242 |
| 0.465 | 168 | 191 | 189 | 183 |

## 2.4. Total counts of gamma rays by using Huawei Ascend P7

The number of counts were counted in 60 seconds and iterated for three times.

| Equivalent Dose Rate (mSv/hr) | 1st | 2nd | 3rd | Average |
|---|---|---|---|---|
| 24.2 | 9512 | 9390 | 9477 | 9460 |
| 6.01 | 2515 | 2506 | 2499 | 2510 |
| 2.61 | 1224 | 1217 | 1206 | 1220 |
| 1.44 | 756 | 775 | 716 | 749 |
| 0.93 | 527 | 503 | 480 | 503 |
| 0.632 | 294 | 266 | 251 | 270 |
| 0.465 | 198 | 184 | 198 | 193 |

## 3. The investigation sensitivity of smartphones by using Co-60

### 3.1 Converting Exposure rate to Equivalent Dose rate

By using the conversion from 2.1.6 1 Sv/hr = 1 Gy/hr = 114 R/hr, we can convert the exposure rate to equivalent dose rate as:

| Exposure Rate (R/hr) | Equivalent Dose Rate (mSv/hr) |
|---|---|
| 1000 | 8810 |
| 560 | 4910 |
| 357 | 3130 |
| 249 | 2190 |
| 183 | 1600 |

| Exposure Rate (mR/hr) | Equivalent Dose Rate (mSv/hr) |
|---|---|
| 32.8 | 0.288 |
| 14.5 | 0.127 |
| 8.13 | 0.071 |
| 5.21 | 0.046 |
| 3.57 | 0.031 |



### 3.2.Total counts of gamma rays by using Samsung Galaxy SII

The number of counts were counted in 30 seconds and iterated for three times (high dose rate of Co-60).

| Equivalent Dose Rate (mSv/hr) | 1st | 2nd | 3rd | Average |
|---|---|---|---|---|
| 8810 | 1645041 | 1645152 | 1640455 | 1640000 |
| 4910 | 928004 | 938483 | 933252 | 933000 |
| 3130 | 586378 | 592624 | 584925 | 588000 |
| 2190 | 400146 | 405923 | 408644 | 405000 |
| 1600 | 292877 | 299888 | 296395 | 296000 |

## 3.3.Total counts of gamma rays by using Samsung Galaxy

The number of counts were counted in 30 seconds and iterated for three times (high dose rate of Co-60).

| Equivalent Dose Rate (mSv/hr) | 1st | 2nd | 3rd | Average |
|---|---|---|---|---|
| 8810 | 1736113 | 1739160 | 1736888 | 1740000 |
| 4910 | 968273 | 968977 | 965427 | 968000 |
| 3130 | 607351 | 607238 | 606602 | 607000 |
| 2190 | 422990 | 423881 | 423783 | 424000 |
| 1600 | 312040 | 313386 | 313033 | 313000 |

The number of counts were counted in 30 seconds and iterated for three times (low dose rate of Co-60).

| Equivalent Dose rate (mSv/hr) | 1st | 2nd | 3rd | Average |
|---|---|---|---|---|
| 0.288 | 54 | 58 | 55 | 55.7 |
| 0.127 | 24 | 26 | 24 | 24.7 |
| 0.071 | 14 | 13 | 13 | 13.3 |
| 0.046 | 8 | 8 | 8 | 8.00 |
| 0.031 | 4 | 5 | 5 | 4.67 |



## 3.4.Total counts of gamma rays by using Huawei Ascend P7

The number of counts were counted in 30 seconds and iterated for three times (high dose rate of Co-60).

| Equivalent Dose Rate (mSv/hr) | 1st | 2nd | 3rd | Average |
|---|---|---|---|---|
| 8810 | 2080932 | 2088884 | 2087041 | 2090000 |
| 4910 | 1142393 | 1145853 | 1144070 | 1140000 |
| 3130 | 723053.5 | 723919 | 721676 | 723000 |
| 2190 | 499284.5 | 499110 | 495800 | 498000 |
| 1600 | 364932 | 364949 | 365381 | 365000 |

The number of counts were counted in 30 seconds and iterated for three times (low dose rate of Co-60).

| Equivalent Dose rate (mSv/hr) | 1st | 2nd | 3rd | Average |
|---|---|---|---|---|
| 0.288 | 77 | 71 | 78 | 75.3 |
| 0.127 | 29 | 29 | 29 | 29.0 |
| 0.071 | 15 | 16 | 15 | 15.3 |
| 0.046 | 12 | 12 | 12 | 12.0 |
| 0.031 | 10 | 10 | 10 | 10.0 |

## 4. Calibration smartphones with Cs-137

### 4.1. Converting Exposure rate to Equivalent dose rate

By using the conversion from 2.1.6 1 Sv/hr = 1 Gy/hr = 114 R/hr, we can convert the exposure rate to equivalent dose rate as:

| Exposure Rate (R/hr) | Equivalent Dose Rate (mSv/hr) |
|---|---|
| 3.39 | 29.7 |
| 1.49 | 13.1 |
| 0.839 | 7.36 |
| 0.535 | 4.69 |
| 0.370 | 3.25 |



### 4.2. Total counts of gamma rays by using Huawei Ascend P7 calibrated with Cs-137

The number of counts were counted in 30 seconds and iterated for three times.

| Equivalent Dose Rate (mSv/hr) | 1st | 2nd | 3rd | Average |
|---|---|---|---|---|
| 29.7 | 6088 | 6057 | 6323 | 6160 |
| 13.1 | 2635 | 2718 | 2694 | 2680 |
| 7.36 | 1529 | 1554 | 1523 | 1540 |
| 4.69 | 1016 | 971 | 915 | 967 |
| 3.25 | 719 | 647 | 651 | 672 |

### 4.3. Total counts of gamma rays by using Samsung Galaxy SIII calibrated with Cs-137

The number of counts were counted in 30 seconds and iterated for three times.

| Equivalent Dose Rate (mSv/hr) | 1st | 2nd | 3rd | Average |
|---|---|---|---|---|
| 29.7 | 4985 | 5095 | 5033 | 5040 |
| 13.1 | 2215 | 2158 | 2203 | 2190 |
| 7.36 | 1157 | 1159 | 1249 | 1190 |
| 4.69 | 749 | 763 | 781 | 764 |
| 3.25 | 553 | 536 | 558 | 549 |

## 5. Calibration Factor

Based on calibration factor equation:

F ((mSv/hr)/cps) = Equivalent Dose Rate (mSv/hr) ÷ Count Rate (cps)

| Equivalent Dose Rate (mSv/hr) | Count rate (cps) by Huawei Ascend P7 | F ((mSv/hr)/cps) |
|---|---|---|
| 29.7 | 205 | 0.145 |
| 13.1 | 89.3 | 0.147 |
| 7.36 | 51.3 | 0.143 |
| 4.69 | 32.2 | 0.146 |
| 3.25 | 22.4 | 0.145 |

So, the average calibration factor is F = 0.145 (mSv/hr)/cps (1)

By using Huawei Ascend P7, we got the number of count rate (cps) as in the table below:

| 1st | 2nd | 3rd | Average | count rate (cps) |
|---|---|---|---|---|
| 109 | 104 | 113 | 109 | 3.62±0.347 |
| 72 | 71 | 76 | 73.0 | 2.43±0.285 |
| 51 | 49 | 46 | 48.7 | 1.62±0.233 |
| 35 | 38 | 37 | 36.7 | 1.22±0.202 |
| 26 | 27 | 29 | 27.3 | 0.911±0.174 |

Finally, the equivalent dose rate of gamma rays by using Huawei Ascend P7 is calculated by the calibration factor equation:

F ((mSv/hr)/cps) = Equivalent Dose Rate (mSv/hr) ÷ Count Rate (cps)

Then Equivalent Dose Rate (mSv/hr) = F ((mSv/hr)/cps) × Count Rate (cps)
The result is shown in the table below:

| count rate (cps) | F ((mSv/hr)/cps) | Equivalent Dose Rate (mSv/hr) |
|---|---|---|
| 3.62 | 0.145 | 0.525 |
| 2.43 | 0.145 | 0.352 |
| 1.62 | 0.145 | 0.235 |
| 1.22 | 0.145 | 0.177 |
| 0.911 | 0.145 | 0.132 |

6. Comparison the Standard Equivalent Dose rate with the Equivalent Dose Rate from Survey Meter and Equivalent Dose Rate from Smartphone (Huawei Ascend P7)

## 6.1. Converting the Exposure rate to Equivalent dose rate

The table below is the converting of standard exposure rate (mR/hr) to equivalent dose rate (mSv/hr):

| Standard Exposure ate (mR/hr) | Equivalent Dose Rate (mSv/hr) |
|---|---|
| 62.1 | 0.545 |
| 39.5 | 0.346 |
| 27.2 | 0.239 |
| 20.1 | 0.176 |
| 15.2 | 0.133 |

Also, the result exposure rate (mR/hr) from survey meter was converted to equivalent dose rate (mSv/hr)

| Exposure Rate (mR/hr) | Equivalent Dose Rate (mSv/hr) |
|---|---|
| 62.4 | 0.547 |
| 39.9 | 0.350 |
| 27.5 | 0.241 |
| 20.1 | 0.176 |
| 15.1 | 0.132 |

# VITA

Sandy Tith was born in Takeo Province, Cambodia, in September 1992. She started with the bachelor program in 2009, major General Chemistry, at Royal University of Phnom Penh (RUPP). In 2013, she became an awardee of the program Young Engineer and Scientist (YES) of Cambodia from the HONDA foundation, Japan. After she received the bachelor's degree in 2013, she got a scholarship from European Commission's CBRN Centers of Excellence to study Master of Science programme on Nuclear Security and Safeguards at the Department of Nuclear Engineering, Faculty of Engineering, Chulalongkorn University.